DETECTION OF FLAWS IN ASPHALT OVERLAID CONCRETE BRIDGE DECKS USING ULTRASONIC GUIDED WAVES

PI: Ece Erdogmus, Ph.D., P.E.

FINAL REPORT

Durham School of Architectural Engineering and Construction

1110 South 67 Street, Omaha, NE 68182

Sponsored By

Nebraska Department of Transportation and U.S. Department of Transportation Federal Highway Administration

December 2020

NEBRASKA
Good Life. Great Journey.
DEPARTMENT OF TRANSPORTATION

THE DURHAM SCHOOL
OF ARCHITECTURAL ENGINEERING AND CONSTRUCTION

TECHNICAL REPORT DOCUMENTATION PAGE

To add text, click inside the form field below (will appear as a blue highlighted or outlined box) and begin typing. The instructions will be replaced by the new text. Only boxes with form fields must be completed.

Please remove this field before completing form.

1. Report No. M086	**2. Government Accession No.** NA	**3. Recipient's Catalog No.**
4. Title and Subtitle Detection of Flaws in Asphalt Overlaid Concrete Bridge Decks Using Ultrasonic Guided Waves		**5. Report Date** December 2020
		6. Performing Organization Code NA
7. Author(s) Ece Erdogmus, PhD, PE		**8. Performing Organization Report No.** NA
9. Performing Organization Name and Address Durham School of Architectural Engineering and Construction University of Nebraska-Lincoln 107 Peter Kiewit Institute (PKI), 1110 S. 67th Street Omaha, NE 68182		**10. Work Unit No.**
		11. Contract SPR-P1(20) M113
12. Sponsoring Agency Name and Address Nebraska Department of Transportation Research Section 1400 Hwy 2, Lincoln, NE 68502		**13. Type of Report and Period Covered** Final Report July 201- December 2020
		14. Sponsoring Agency Code

15. Supplementary Notes

If applicable, enter information not included elsewhere, such as translation of (or by), report supersedes, old edition number, alternate title (e.g. project name), or hypertext links to documents or related information.

16. Abstract

This paper presents the results from laboratory experiments to determine the capabilities of a recently developed nondestructive testing (NDT) approach for detecting the flaws at the asphalt-membrane-concrete layers and rebar-concrete interfaces for asphalt-overlaid reinforced concrete bridge decks. The novel Ultrasonic Guided Wave Leakage (UGWL) method previously developed by University of Nebraska-Lincoln (UNL) and Nebraska Department of Transportation (NDOT) utilizes the steel rebar as a wave guide by placing an ultrasound transmitter at the rebar and measures the leaked energy from the top surface of concrete (or asphalt) with an array of ultrasonic receivers. This method has proved successful previously as a continuous monitoring tool in lab experiments, where early rebar-concrete delaminations as small as 0.008", and early corrosion in specimens soaked in salt-water (as early as 9 days) have been detected in various configurations and sizes of reinforced concrete specimens. Further, two proof-of-concept studies for instantaneous field testing has been carried out. First, on an existing bridge, concrete was cored to the top rebar level and a transmitter was attached to the rebar and an array of readings were taken from the concrete surface in 6 inch increments up to 14 feet from the transmitter. While the attenuation curve from this test was as expected based on theory of ultrasonic guided waves, without a baseline data from previous years, such data is difficult to interpret for accurate flaw detection. In the second field application, a transmitter was attached on a rebar during construction and embedded in concrete. Several months of testing showed no significant change, as expected, but this experiment proved that the attachment was secure and durable in field conditions. Future readings from this field implementation can reveal change in the condition of this bridge deck since baseline data does exist in this case. None of these systems (lab or field) included asphalt overlay, therefore this latest phase of the project aimed to explore the method's capabilities when the deck is overlaid with asphalt for wider spectrum of applications. Several asphalt-overlaid reinforced concrete laboratory specimens were tested in this study and the results showed that with careful placement of sensors and data analysis, flaws at the membrane level as well as the rebar level could be successfully detected. As stated before, the UGWL method's strength lies in continuous monitoring: change in amplitudes from a baseline data is more meaningful than instantaneous amplitude readings at this time. This method has the potential to answer an important need in infrastructure quality control and maintenance; namely *membrane inspections to detect construction flaws*.

17. Key Words	**18. Distribution Statement**
Nondestructive tests, corrosion tests, corrosion, reinforced concrete bridges, ultrasonic tests, ultrasonic waves	No restrictions. This document is available through the National Technical Information Service. 5285 Port Royal Road, Springfield, VA 22161

19. Security Classification (of this report)	**20. Security Classification (of this page)**	40	**22. Price**
Unclassified	Unclassified		

Form DOT F 1700.7 (8-72) Reproduction of completed page authorized

DISCLAIMER

The contents of this report reflect the views of the authors, who are responsible for the facts and the accuracy of the information presented herein. The contents do not necessarily reflect the official views or policies neither of the Nebraska Department of Transportations nor the University of Nebraska-Lincoln. This report does not constitute a standard, specification, or regulation. Trade or manufacturers' names, which may appear in this report, are cited only because they are considered essential to the objectives of the report.

The United States (U.S.) government and the State of Nebraska do not endorse products or manufacturers. This material is based upon work supported by the Federal Highway Administration under SPR-P1(20) M113. Any opinions, findings and conclusions or recommendations expressed in this publication are those of the author(s) and do not necessarily reflect the views of the Federal Highway Administration."

Contents

ABSTRACT

This paper presents the results from laboratory experiments to determine the capabilities of a recently developed nondestructive testing (NDT) approach for detecting the flaws at the asphalt-membrane-concrete layers and rebar-concrete interfaces for asphalt-overlaid reinforced concrete bridge decks. The novel Ultrasonic Guided Wave Leakage (UGWL) method previously developed by University of Nebraska-Lincoln (UNL) and Nebraska Department of Transportation (NDOT) utilizes the steel rebar as a wave guide by placing an ultrasound transmitter at the rebar and measures the leaked energy from the top surface of concrete (or asphalt) with an array of ultrasonic receivers. This method has proved successful previously as a continuous monitoring tool in lab experiments, where early rebar-concrete delaminations as small as 0.008", and early corrosion in specimens soaked in salt-water (as early as 9 days) have been detected in various configurations and sizes of reinforced concrete specimens. Further, two proof-of-concept studies for instantaneous field testing has been carried out. First, on an existing bridge, concrete was cored to the top rebar level and a transmitter was attached to the rebar and an array of readings were taken from the concrete surface in 6 inch increments up to 14 feet from the transmitter. While the attenuation curve from this test was as expected based on theory of ultrasonic guided waves, without a baseline data from previous years, such data is difficult to interpret for accurate flaw detection. In the second field application, a transmitter was attached on a rebar during construction and embedded in concrete. Several months of testing showed no significant change, as expected, but this experiment proved that the attachment was secure and durable in field conditions. Future readings from this field implementation can reveal change in the condition of this bridge deck since baseline data does exist in this case. None of these systems (lab or field) included asphalt overlay, therefore this latest phase of the project aimed to explore the method's capabilities when the deck is overlaid with asphalt for wider spectrum of applications. Several asphalt-overlaid reinforced concrete laboratory specimens were tested in this study and the results showed that with careful placement of sensors and data analysis, flaws at the membrane level as well as the rebar level could be successfully detected. As stated before, the UGWL method's strength lies in continuous monitoring: change in amplitudes from a baseline data is more meaningful than instantaneous amplitude readings at this time. This method has the potential to answer an important need in infrastructure quality control and maintenance; namely *membrane inspections to detect construction flaws*.

Keywords: Nondestructive testing, ultrasonic guided waves, asphalt, reinforced concrete bridge decks, structural health monitoring

1. INTRODUCTION

This paper presents the findings regarding the application of a recently developed ultrasonic guided wave-based method on asphalt overlaid reinforced concrete laboratory specimens. This work is a part of a multi-phase study conducted at the University of Nebraska-Lincoln (UNL) in collaboration with the Nebraska Department of Transportation (NDOT).

The recently developed method involves use of the steel reinforcement as a wave guide that transmits the ultrasonic waves through the system and the measurement of the leaked energy at the surface of the concrete. Hence, the approach is named ultrasonic guided wave leakage (UGWL) method. The leaked ultrasonic wave data is collected from an array of receivers on the top surface of the system and it is processed in the frequency domain. While the instantaneous or single reading of the data may not be easy to interpret, significant changes in the amplitude over time present clear indications of changes in the condition of the system. This method provides a significant improvement over conventional damage assessment techniques, detecting microcracking and minor corrosion effects before corrosion and/or delamination has progressed to a damaging level. In the previously published phases of this study, first, the proof of concept for the proposed UGWL method's effectiveness to detect the onset of delamination in reinforced concrete was demonstrated successfully (Garcia et al., 2017). Then, early detection of the onset of corrosion and cracking in concrete was also demonstrated and improvements are made to the process in terms of attachment of the transmitter to the rebar and subsequent field trials (Garcia et al., 2019 and Erdogmus et al., 2020).

This paper presents the findings from laboratory tests on asphalt only and asphalt-reinforced concrete specimens in order to expand the application of the novel method. Therefore, the ultimate goal of this particular phase of the study is to understand the applicability of the novel method and its variations, including the traditional ultrasonic pulse velocity technique, to asphalt-overlaid reinforced concrete (RC) when additional layers (primer, membrane, and asphalt) are added to the system. The objectives to achieve this goal include:

1. To determine the effects of the asphalt overlay on the ultrasonic testing methods to detect flaws at rebar-concrete interface
2. Understand to what extent, the flaws at the asphalt-membrane-concrete interface can be detected using ultrasonic testing methods

2. BACKGROUND

There is an increased demand for structural health monitoring (SHM) systems for the rapidly aging U.S. infrastructure. Steel reinforcement is used in most of these concrete structures including buildings, bridges, and parking structures. Due to the corrosion potential of the steel reinforcement, problems such as delamination and spalling occur and, if left untreated, they lead to adverse effects to the integrity and structural capacity of the overall structure. Reinforced concrete bridge decks are particularly susceptible to corrosion and delamination due to the harsh conditions they commonly experience including freeze-thaw cycles, de-icing salts, continuous impact from heavy traffic, and exposure to water. It has been estimated that the annual corrosion related repair costs for highway bridges exceeds $8.3 billion. This includes $2 billion for bridge deck repairs (Cui, 2012), with corrosion and delamination accounting for approximately 40 percent of these cost (Yunovich et al., 2001).

Due to these concerns about rebar corrosion and related problems, NDOT routinely provides additional corrosion resistance to bridge decks by placing a waterproof membrane with an asphalt overlay to reinforced concrete bridge decks either immediately or within 10 years of construction. With the addition of a primer, water proof membrane, and asphalt layers, water and salt is less likely to reach the rebar and cause corrosion. However, imperfect placement of the membranes is known to be a common occurrence

by departments of transport (DOTs) and *better methods for the quality control for these membranes* and/or *condition assessment of the rebar-concrete interface are both high priority research needs.*

Corrosion can lead to delamination when left unmanaged. As explained in further detail in Garcia et al., (2019), chemical delamination forms the first stage of corrosion-related deterioration. These initial stages of corrosion temporarily improve the bond between concrete and steel. As corrosion continues to develop, formation of iron oxides at the steel surface results in significant volumetric increase. This in turn creates internal pressures at the steel-concrete interface, and once the internal pressures cause the concrete to experience great enough tensile stresses, mechanical delamination is experienced. The UGWL method has proved successful in detection of the onset of corrosion as well as very small widths of delamination (0.008 inches) as explained in Garcia et al.(2017), Garcia et al.(2019), and Erdogmus et al., (2020). This particular project aims to expand the application of this recently developed method to asphalt-overlaid systems.

Several others looked at use of ultrasonic testing mostly to assess the condition of the asphalt with respect to cracking, oxidation, and aging. Kalyoncuoglu et al. (2004) used ultrasonic testing for fatigue life estimation for asphalt concrete. Khazanovich et al. (2005) evaluated the cracks in asphalt while Khazanovich et al. (2012) aimed to detect delamination in asphalt pavements, both using traditional ultrasonic testing techniques. Haser et al. (2015) monitored viscosity in asphalt binders using ultrasonic guided waves. They use a lab setup with an asphalt specimen placed in a vacuum, and they focus on the torsional waves. With this, they ensure that the energy will not leak from the waveguide (rod) and attenuation is due solely to material absorption. This is a contrasting objective to ours, where we utilize the leaked energy and therefore we do want that energy transfer. Further, while we utilize shear and longitudinal waves in the leaked energy (in UGWL method) or the direct ultrasonic energy (in the UPV method) mostly, Haser et al.'s work focuses on isolated torsional waves. Pahlavan et al. (2016) looked at the influence of asphalt on fatigue crack monitoring in steel bridge decks using guided waves. While this is also a guided wave study, their experimental setup, aims, and materials involved are vastly different. Their aim is to find and size cracks at the welded connections of stiffener elements in steel bridge decks that eventually propagate to the asphalt layer. They also make the point, as we do, that ultrasonic testing can help find these issues before they become significant problems. This experimental setup involves an array of transmitters and receivers on the steel deck and use the deck as the wave guide. It should also be mentioned that the description of asphalt installation is vastly different in this study originated in Netherlands than that is in Nebraska. They utilize alternating pairs of two membranes and two asphalt layers in a configuration called "open-surface asphalt". Their study is helpful to ours in benchmarking the asphalt-related quicker attenuation of the ultrasonic waves we have also observed, but other than this, direct parallels are difficult to form between their study and ours. Zargaret al. (2017) is another study that focused solely in the assessment of asphalt using ultrasonic testing, where theyused ultrasonic wave transmission techniques to evaluate air voids in asphalt. Finally, McGovern et al. (2018) published a review on their former studies related to the evaluation of asphalt pavements using noncollinear Ultrasonic Wave Mixing. In their study, they use three transmitters at different positions and angles to the specimen to create three rays of waves to be mixed and then processed to determine the aging and oxidation in small lab samples of asphalt concrete. This nonlinear acoustic approach, in the form of a noncollinear wave mixing technique, involves the mixing of two ultrasonic waves to produce a third, nonlinear scattered wave. They also recommend rejuvenators to maintain the health of the asphalt mixes.

These studies have been beneficial in benchmarking some of the findings from this work, such as the faster attenuation of ultrasonic waves in asphalt compared to other materials (such as concrete) found by Pahlavan et al. (2016), which agrees with our findings. However, even the studies that have utilized guided waves in some way have vastly different experimental setups, goals, and applications. None of these studies attempted to use a rebar placed in the asphalt layer or the rebar in the concrete below the asphalt layer as a wave guide to detect flaws at the membrane level and/or rebar-concrete level. Further, when they utilized guided waves, they aimed to minimize the leakage to the surrounding materials while

we aim to take advantage of the leakage and measure the leaked energy rather than the direct attenuated ultrasonic waves.

3. METHODS, MATERIALS, AND SPECIMENS

In this section, the standardized Ultrasonic Pulse Velocity (UPV) method and the recently developed UGWL method will be briefly presented, followed by the introduction of the three sets of laboratory test specimens.

In previous work on this project, tested assemblies were reinforced concrete, as such the surrounding material was only concrete (Garcia et al., 2017; Garcia et al., 2019, and Erdogmus et al.,2020). With the addition of asphalt, depending on the specimen and objective of the specific test, the transmitter is placed on the rebar (UGWL method) *or* the asphalt (UPV method); and the receivers are placed on the asphalt surface. The ultrasonic testing device used in this study is the Pulsonic Ultrasonic Pulse Analyzer 58-E4900 from Controls Group. Standard 54 kHz transducers with a 2-inch dimeter are used as the transmitter and receiver.

3.1. UPV Method

UPV is the standardized method of ultrasonic testing of concrete and it is used to assess the quality of concrete and to identify the presence of voids and cracks. Pulses of longitudinal stress waves are generated by an electro-acoustical transducer that is held in contact with one surface of the concrete under test. After traversing through the concrete, the pulses are received and converted into electrical energy by a second transducer located a distance (L) from the transmitting unit. The transit time (T) is measured electronically. The pulse velocity (V) is calculated by diving L by T (Equation 1). V related to properties of concrete as shown in Equation 2. (ASTM 597).

$$V = \frac{L}{T} \qquad \text{[Eq.1]}$$

$$V = \sqrt{\frac{E(1-\mu)}{\rho(1+\mu)(1-2\mu)}} \qquad \text{[Eq.2]}$$

where,
E = dynamic modulus of elasticity,
μ= dynamic Poisson's ratio, and
ρ= density

The typical and standardized layout for UPV is the "direct measurement technique" shown in Figure 1. The distance traveled, L, refers to the thickness of concrete in this setup. Other setups (semidirect and indirect) in Figure 1 are also referenced by ASTM C597, with the caveats that the results will be different than the direct measurements and they will likely be indicative only of surface layers. The standard acknowledges that in the case of indirect measurements, there is uncertainty in determining the actual length of the travel paths of the pulses and that the use of Equation 1 will be difficult or lead to errors. However, use of an array of sensors equally spaced to compare to one another is offered as a solution and this approach is utilized for Specimen B in this study.

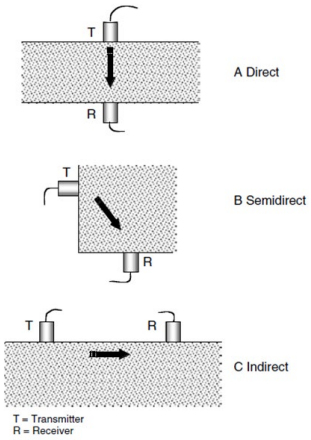

Figure 1. Transmitter and Receiver arrangements in UPV

3.2. UGWL Method

Figure 2 illustrates the UGWL method previously developed by the first author and her team (Garcia et al. 2017; Garcia et al., 2019; and Erdogmus et al., 2020) for assessment of condition of the rebar, rebar-concrete interface, and concrete. In the UGWL experimental set-up, a transmitter (T) is placed at the end of a steel rebar sending the energy directly and longitudinally into the wave guide (rebar). A receiver (R) is placed on the external top surface. The receiver is moved along the length of the specimen right above the rebar in 6-inch intervals in order to plot the attenuation of the energy across the system's length and to record any deviations from the expected attenuation in the amplitudes of energy leaked into the surrounding material. The longitudinal waves travel through the wave guide and some of the energy leaks into the surrounding medium, depending on the bond between the rebar and the medium as well as existence of other anomalies.

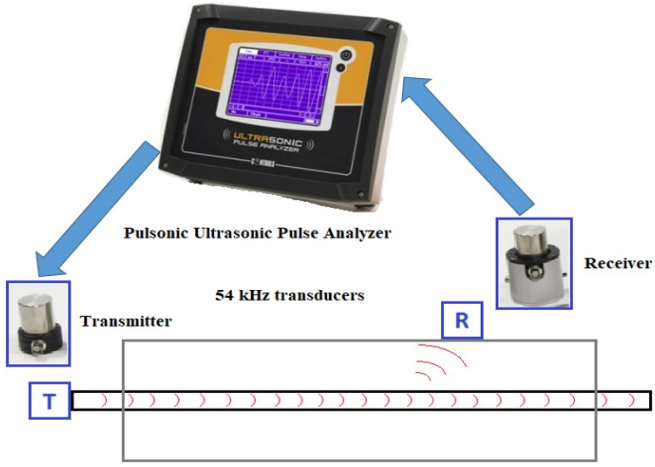

Figure 2. Experimental Setup

3.3. Laboratory Specimens

Three sets of specimens were studied at the UNL Structures Laboratory in Omaha, Nebraska. Following sections explain these specimens.

Specimen Set A: Asphalt Only Specimens

Two asphalt specimens measuring 3 ft x 3ft x 4 in. constitute Specimen Set A. Specimen A1, shown in Figure 3 is composed entirely of asphalt and its purpose is to isolate the wave propagation properties of asphalt with indirect UPV measurements. Specimen A2 includes a #4 rebar in the center to be utilized as the wave-guide (Figure 4). The purpose of Specimen A2 is to compare the UGWL method's application in asphalt to previous findings with reinforced concrete specimens. A primer (Polyguard 650 RC Liquid Adhesive solution) was applied on the surface of the bottom plywood (Figures 3a and 4a) as well as the Polyguard 665 Membrane (Figure 4b) before the hot asphalt mix was placed and hand-compacted (Figure 3b). After the casting, the asphalt is left inside the formwork to maintain its integrity throughout the data collection process (Figures 3c and 4c).

(a) (b) (c)

Figure 3. Specimen A1 (Asphalt only): (a) Primer Application, (b) Compaction, (c) Cast Specimen

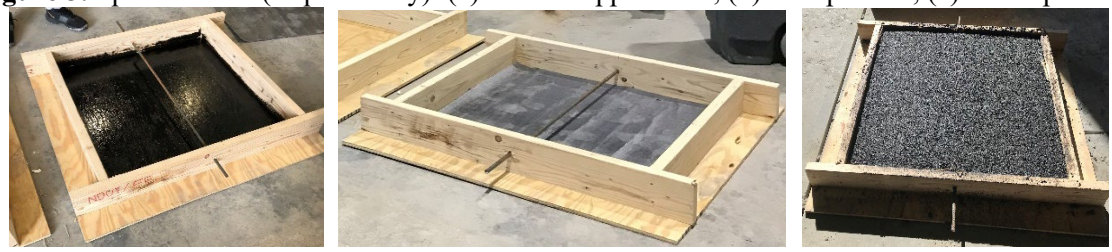

(a) (b) (c)

Figure 4. Specimen A2 (Asphalt with rebar): (a): Primer, (b) Membrane, (c): Cast Specimen

Specimen Set B: Embedded Flaws at the Membrane Level

This set includes a single specimen with various flaws embedded at the membrane level (immediately underneath the membrane). A blown-up image of Specimen B is shown in Figure 5. For this specimen, first a concrete slab is cast with a single longitudinal reinforcement and six transverse rebars. After curing the concrete slab for 28 days, the primer, membrane, and the asphalt are placed. The membrane is divided into five areas (B1-B5). The first segments from both ends (B1 and B5) are considered "perfect membrane", where care is taken to place the membrane according to NDOT and manufacturers' specifications. Three middle segments (going from right to left on Figure 5) include different flaws embedded underneath the membrane, as shown in Figure 6:

- *B2- Gravel under the membrane:* To simulate a typical construction flaw, gravel was dispersed under the membrane in this segment.
- *B3- Air bubbles under the membrane:* This potential construction flaw was simulated by placing a bubble wrap under the membrane. It was considered that the wrap might melt during the hot asphalt casting but the air bubbles would remain.
- *B4- Moisture trapped under the membrane:* This potential construction flaw was simulated by wetting a thick paper towel and placing under the membrane.

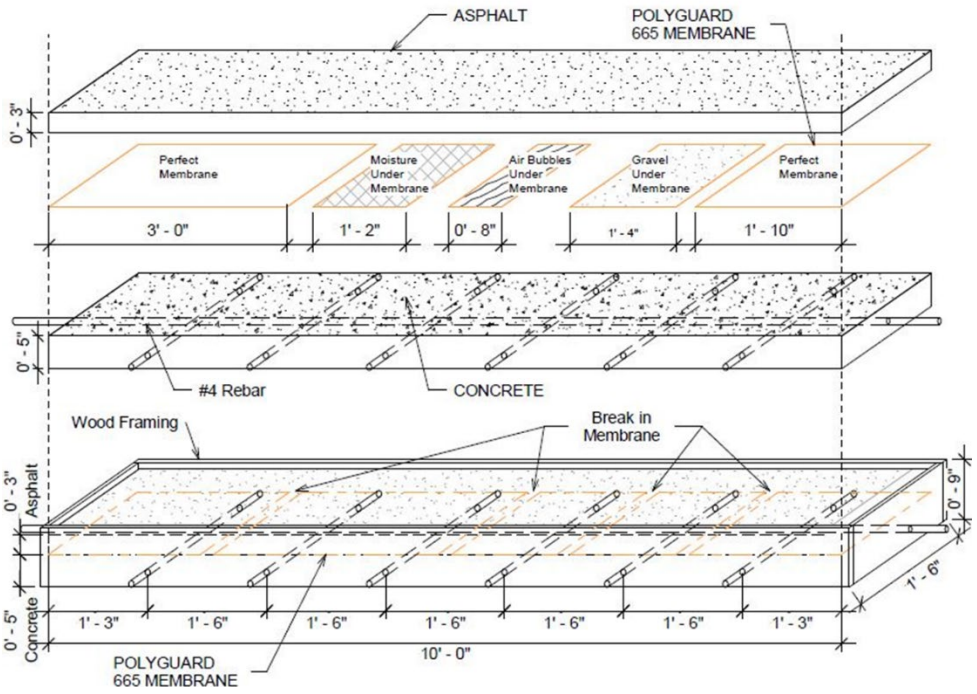

Figure 5. Blown-up Illustration of Specimen B: Various Flaws Embedded at the Membrane Level (Note that the data is collected starting from the right end, therefore Segments B1 is the right-most segment, and B5 is the left-most in the following discussions.)

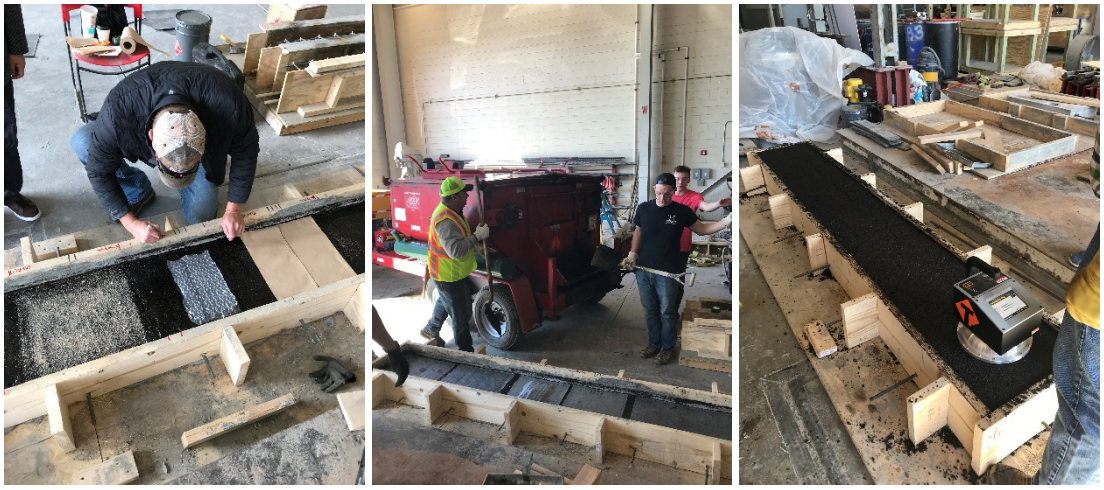

(a) (b) (c)

Figure 6. (Casting of Specimen B: **(a)** Placement of gravel (B2), bubble wrap (B3), and paper towel (B4) between primer and membrane; **(b)** Image after membranes are placed; **(c)** *In-situ* Density measurements

Specimen Set C: Older Concrete Slab under the Asphalt

Three specimens were included in this set.

- *C1 (0-degree bar end and corroded rebar):* Rebar's end was left as is (0-degree) for UGWL measurements (Figure 7). This specimen was soaked in NaCl solution for a period of six months and the bar was corroded. After this period, the asphalt was added (Figure 7a) and ultrasonic testing was performed. Once all testing was done, chloride testing was performed on the concrete

from three cores of this specimen for a parallel study published elsewhere (Amiri 2020 and Amiri et al., 2020).

- C2 *(33-degree bar end and clean rebar):*: Rebar's end was cut to 33-degrees to study the impact of the angle of emitted ultrasonic waves and the rebar is not exposed to any corrosion-accelerators (i.e. clean bar) as shown in Figure 8.
- *C3 (45-degre bar end and clean rebar):* Similar to C2 except the rebar's end was cut to 45-degrees (Figure 9).

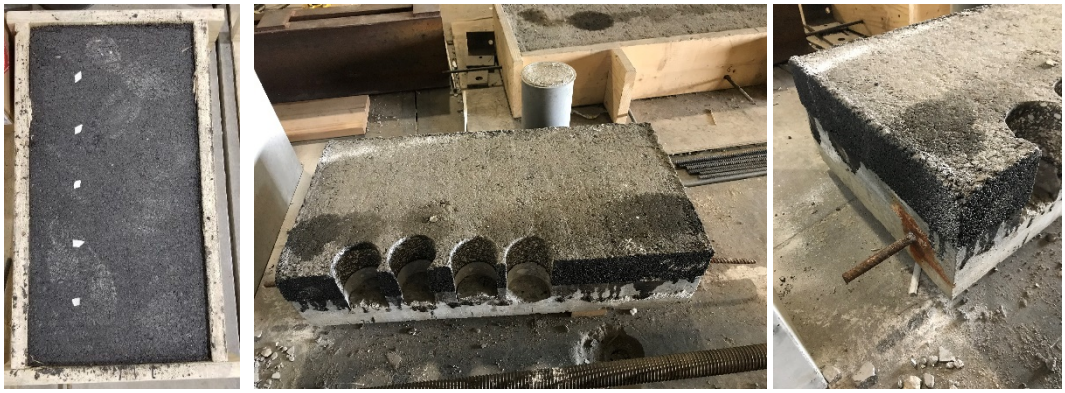

Figure 7. Images of Specimen C1: (a) After asphalt is cast, points show where receivers were placed in testing, (b) After the formwork is stripped and chloride testing is performed (cite paper), (c) Close-up of the corroded blunt-end (0-degree) rebar.

Figure 8. Images of Specimen C2 (33-degree end clean rebar)

Figure 9. Images of Specimen C3 (45-degree end clan rebar)

Asphalt Properties

NDOT Asphaltic Concrete Type SLX (4.75mm) was used to cast these specimens. This mixture is identified by 50 Gyrations and 5.8% Binder. Due to specimen size, a vibratory roller was not used to compact the asphalt. Instead, a vibratory plate compactor and hand tampers were employed. The hand tampers proved to be the most effective tools for this type of placement. Once compaction was optimized, the specimens were allowed to cool. Then, density readings were taken to ensure adequate and uniform compaction through the conventional compaction methods utilized. The final in-place densities were measured and recorded using a non-nuclear testing device and a correction factor for this type of mix (Type SLX) was used to establish approximate values (Table 1).

Table 1. Approximate Asphalt Density Results from In-situ Measurements on Hot Asphalt

Specimen	In-Place Density (lbs/ft³)	Density (%Gmm)
A1 (Asphalt only)	142.4	93.7
A2 (Asphalt with Rebar)	140.6	92.5
B1 (Perfect membrane- end1)	141.3	93.0
B2 (Gravel)	142.2	93.6
B3 (Air bubble)	142.4	93.7
B4 (Moisture under membrane)	141.3	93.0
B5 (Perfect membrane- end2)	141.8	93.3
C1	143.2	94.2
C2	143.9	94.7
C3	143.3	94.3

Later, three cores taken from Specimens A and C, and rectangular pieces were cut from Specimen B (for autopsy, see Section 4.2). These samples were used to confirm the density of the asphalt in each case. Laboratory testing for densities was performed by NDOT personnel Mike Reynolds to confirm the in-place density (See Figures 10-13 and Table 2).

Table 2. Density Results from testing of Core Samples

Specimen		Core Density (lbs/ft³)	Core Density (%Gmm)
A1 (Asphalt Only)			
	A1-1 Core	143.4	94.1
	A1-2 Core	143.9	94.4
	A1-3 Core	142.6	93.5
	Average	**143.3**	**94.0**
A2 (Asphalt with Rebar)			
	A2-1 Core	142.5	93.5
	A2-2 Core	142.4	93.4
	A2-3Core	142.7	93.6
	Average	**142.5**	**93.5**
B1 (Perfect Membrane-end1)		144.0	94.5
B2 (Gravel)		144.3	94.7
B3 (Air Bubble)		144.1	94.5
B4 (Moisture Under Membrane)		142.9	93.7

B5 (Perfect Membrane-end 2)		142.4	93.4
C1			
	C1-1 Core	144.7	94.9
	C1-2 Core	144.5	94.8
	C1-3 Core	144.5	94.8
	Average	**144.5**	**94.8**
C2			
	C2-1 Core	144.0	94.4
	C2-2 Core	144.8	95.0
	C2-3 Core	144.9	95.1
	Average	**144.6**	**94.8**
C3			
	C3-1 Core	148.1	97.2
	C3-2 Core	148.1	97.2
	C3-3 Core	147.2	96.6
	Average	**147.8**	**97.0**

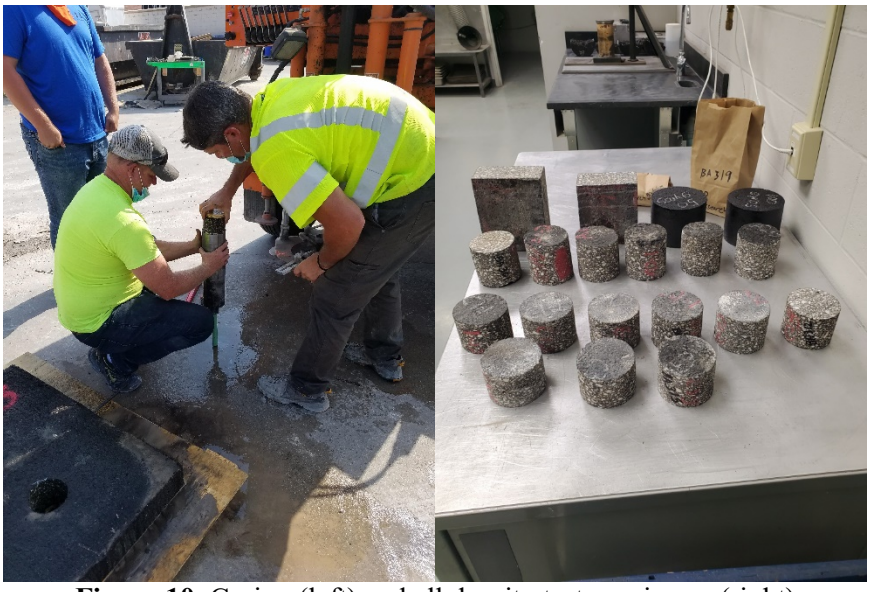

Figure 10. Coring (left) and all density test specimens (right)

Figure 11. Density Test Cores for A Specimens

Figure 12. Density test was conducted on the sliced segments of Specimen B

Figure 13. Density Test Cores for C Specimens

3.4. Field Specimen: Old Bridge Deck Segment

A segment cut from of an asphalt-overlaid reinforced concrete bridge deck was brought to the lab for another NDOT project by UNL faculty Dr. Jingying Zhu (Figure 14). With permission, one of these field specimens was tested in order to investigate if the visually identified condition differences between rebars can also be detected using the UGWL approach. This segment has 9 rebars on the top layer and based on the inspection from the two sides they are all in various levels of deterioration, which will be

discussed in more detail along with the test results, later in this paper. Out of the 9 bars, 5 of them were tested (2, 4, 6, 8, and 9) both from the north end and south end.

Figure 14. Old Bridge Deck Specimen, Left: North End, Right: South End

4. RESULTS AND DISCUSSION

The results of the UGWL method application on the three sets of laboratory specimens and one field specimen are presented in the subsequent sections.

4.1. Specimen Set A Results

Figures 15 and 16 present the results for Specimen A1 and A2, respectively. It should be noted that when there is no rebar and the transmitter is placed on asphalt for Specimen A1, the test method becomes indirect UPV testing (Figure 1) and there is one less receiver in the array. When the data from the first testing point are compared UPV gives an order of magnitude weaker response (0.0014 versus a 0.016) than that of the UGWL method. As such, with amplitudes 10 times higher, this once again proves, in general, that UGWL method provides higher sensitivity in measurements.

There are two reasons for the energy loss between Specimen A1 and A2. First is the difference in methodology. With Specimen A2, UGWL could be applied where the rebar is used as the wave-guide. In the UGWL method, powerful longitudinal waves are generated due to the direction of the transmitter parallel to the direction of propagation. As the wave propagates through the bound element, i.e. the steel rebar (wave guide), the leakage into the surrounding asphalt is measured from the surface of the specimen. The attenuation curve in Figure 16 has a defined exponential decay and confirms that UGWL method can be successfully applied to asphalt if there is a bound element, like steel rebar, in the asphalt.

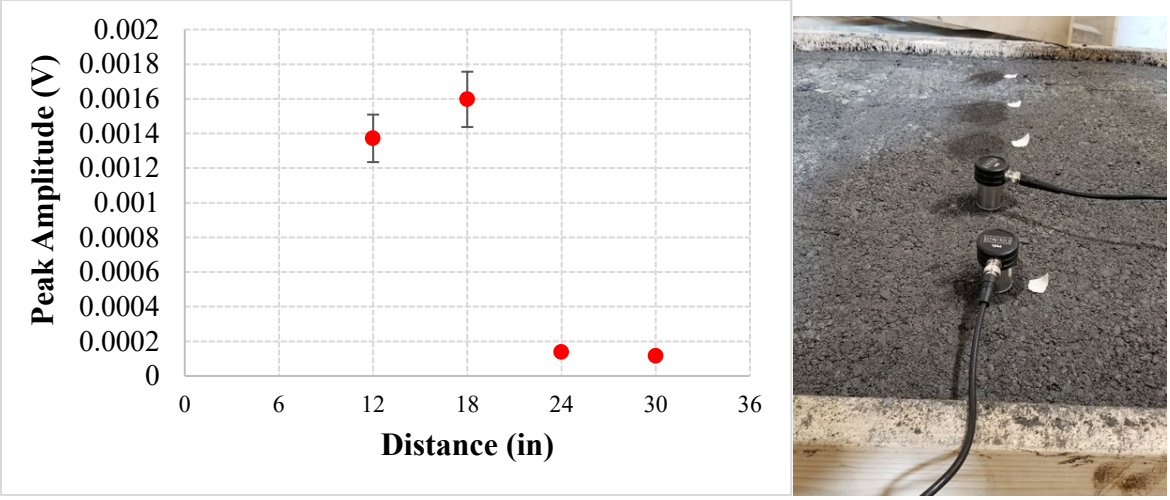

Figure 15. Specimen A1 Results (Asphalt only) and Test Setup (Indirect UPV)

The second reason of the difference is the difference in material properties between asphalt and concrete. Figure 17 shows the UGWL wave attenuation in a reinforced concrete slab. When this is compared to Specimen A2 in Figure 16, it can be seen that there is nearly an order of magnitude difference overall due to the difference in material properties between concrete and asphalt. The faster attenuation in asphalt due to its relevant material properties (see Equation 2) has also been reported by others (Pahlavan et. al, 2016).

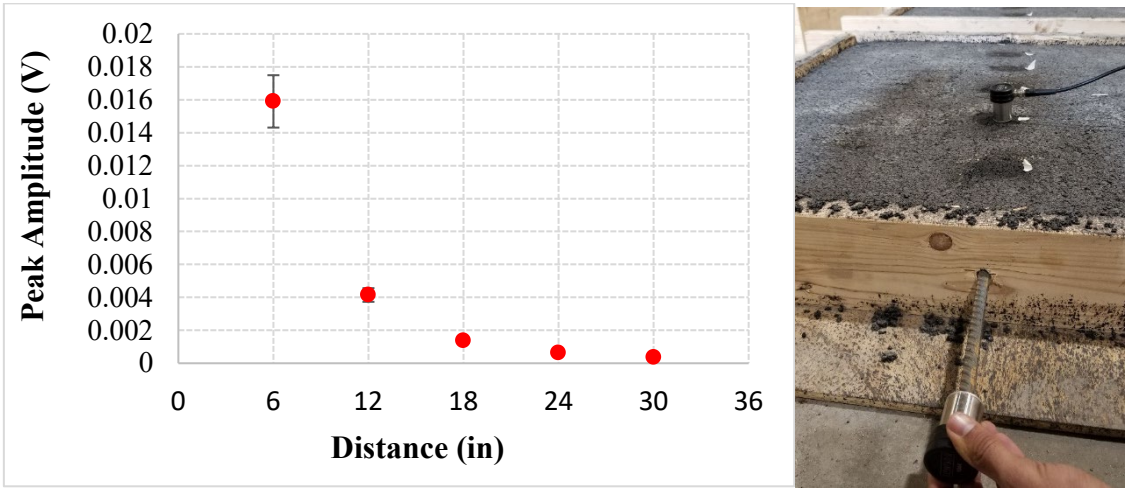

Figure 16. Specimen A2 Results (Asphalt and rebar) and Test Setup (UGWL)

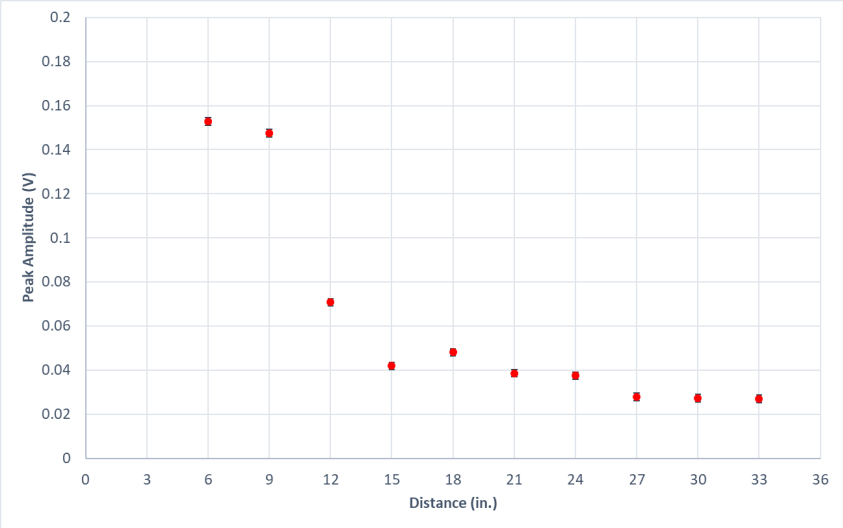

Figure 17. Results from a previous reinforced concrete specimen for comparison to Figure 16. Attenuation in Concrete when the waves are emitted through the rebar in the center of the specimen

Overall, Specimen Set A results show that the UGWL method can still be applied in asphalt-only specimens, especially if a linear thin steel element were to be inserted into the asphalt for testing purposes; but the length of the effective testing range is shorter compared to reinforced concrete specimens. When applied from the surface using the indirect UPV method, further decrease in the amplitudes are observed. However, with surface-only location of both the transmitters and the receivers, the UPV method becomes truly nondestructive and much more practical. The value of the method, therefore, comes down to the question of whether flaws inside the asphalt-overlaid bridge decks can be detected with the indirect UPV method. This question is answered with Specimen Set B.

4.2. Specimen Set B Results

Specimen B involves various known flaws inserted at the membrane level (Figures 5 and 6) and its purpose is to study the potential of the ultrasonic testing in identifying membrane placement errors that are common during construction. Specimen B was tested in four different ways: Longitudinal continuous readings with the UGWL method, longitudinal continuous readings using the indirect UPV method, UGWL method using the transverse bars as the wave guide, and segment-by-segment indirect UPV testing.

Longitudinal Continuous Readings with UGWL and UPV Methods

Figure 18 shows the two continuous tests performed in the long direction first with the transmitter placed on the rebar end (UGWL method) and then the transmitter placed on the asphalt surface roughly 2 inches from the end (Indirect UPV method). The resulting data are presented in Figures 19-21.

(a) (b)

Figure 18. Two longitudinal continuous test setups: (a) UGWL Method application. Transmitter on the end of rebar and receivers along the middle line on the asphalt surface *(Results in Figure 19*). (b) Indirect UPV Application. Transmitter on the asphalt surface 2 inches from the edge and receivers along the middle line on the asphalt surface (*Results in Figures 20-21*).

It must be reiterated that the significant difference in the first amplitudes of these two tests is due to the fundamental difference in the application of the ultrasonic waves, which is illustrated in Figure 22.

In Figure 19 showing the UGWL method application results, the data appears to follow an expected attenuation curve, with the exception of the following locations: at 24 in., at 42 in., a very small increase at 66 in., and the segment spanning between 90- and 114-inches indicating anomalies at these points.

When the indirect UPV method is applied and the full spectrum is plotted as shown in Figure 20, the attenuation from the first data point to the second is so large that it is difficult to make meaningful observations. However, when the first data point is eliminated (therefore zooming into the rest of the data) as shown in Figure 21, not only the amplitudes become similar to those of UGWL, but also fluctuations indicative of anomalies can be observed at the following locations: at 24 in., 36-42 in., at 66 in., at 90 in., and 108-114 in. Therefore, both methods indicate potential of anomalies at similar locations. The corresponding anomalies in these locations are discussed further in conjunction with the segment-by-segment analysis of Specimen B.

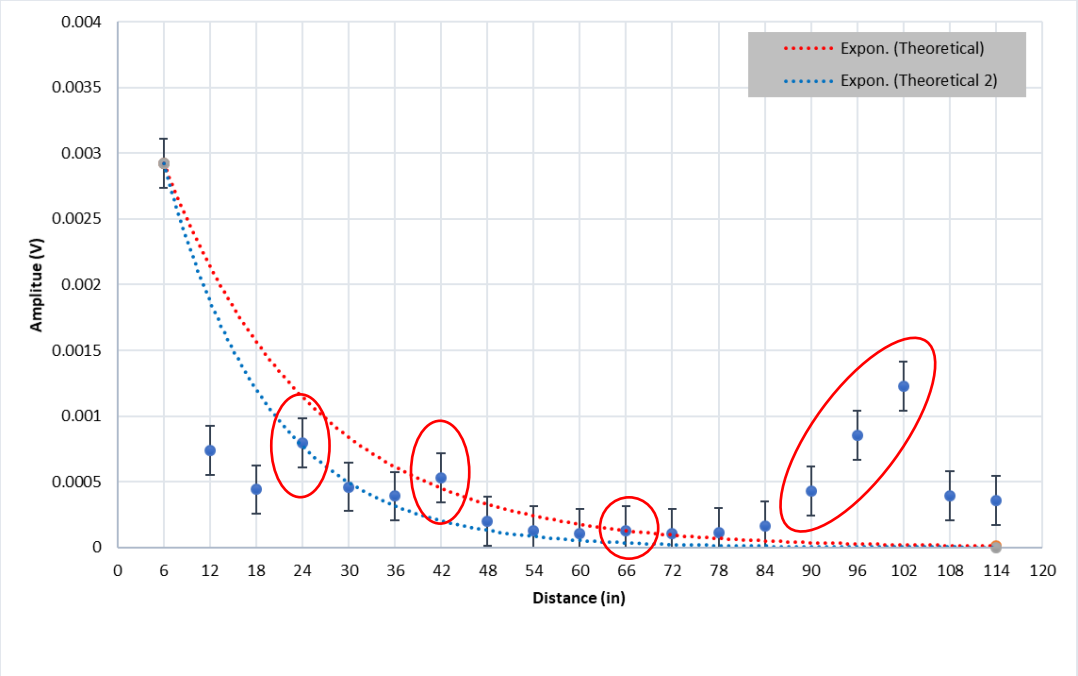

Figure 19. Specimen B- UGWL Results: Transmitter on the rebar end, continuous measurements from the surface of the asphalt

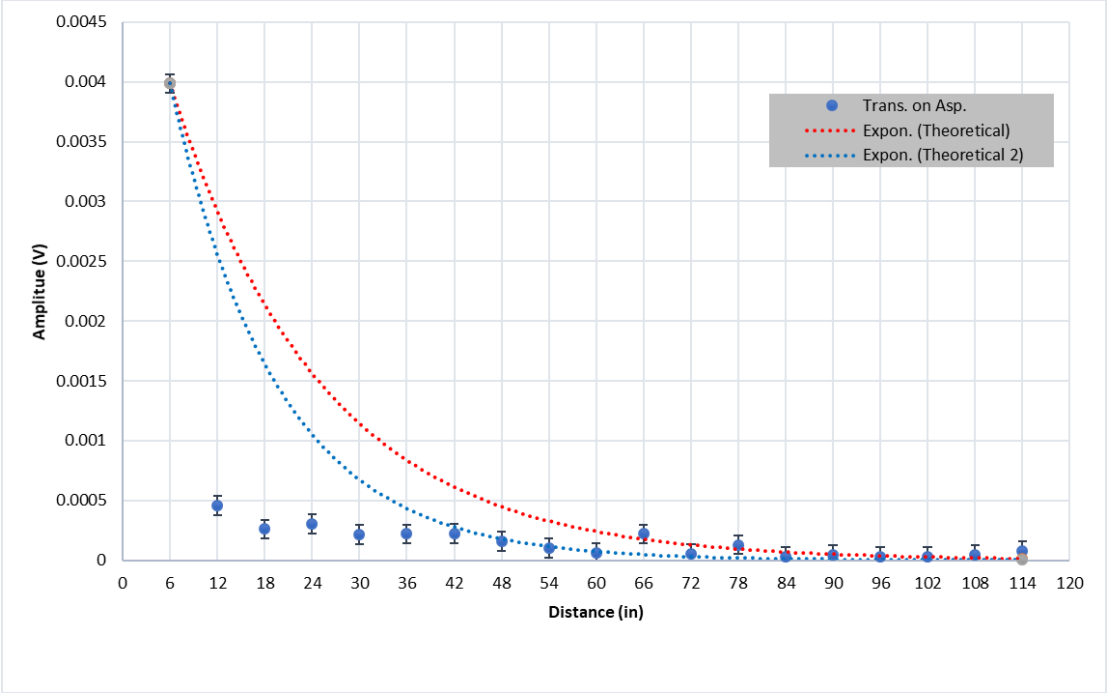

Figure 20. Specimen B -Indirect UPV Results: Transmitter on the asphalt, continuous measurements from the surface of the asphalt

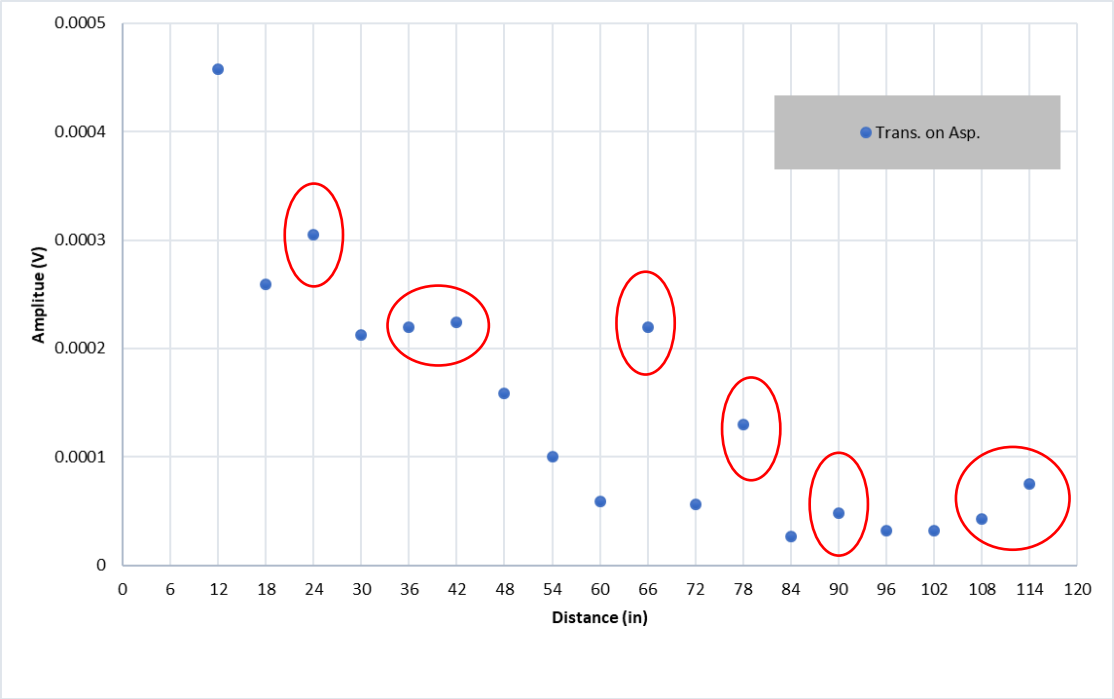

Figure 21. Specimen B- Indirect UPV Results without the first (high amplitude) point data at 6 inches

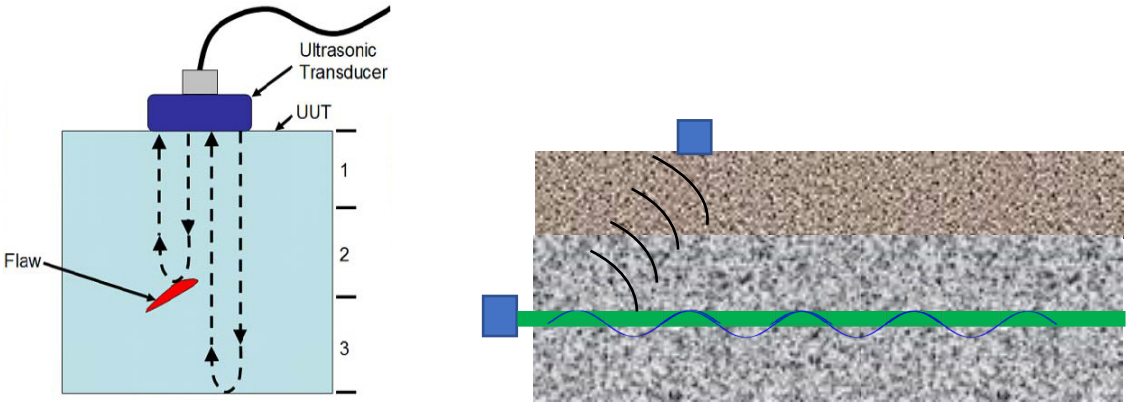

(a) (b)

Figure 22. Left: Traditional Ultrasonic Pulse Velocity Method, Right: Proposed UGWL Method

UGWL Method Using the Transverse Bars

As can be seen in Figures 5 and 6, Specimen B includes six transverse bars and they are numbered 2-7, counting the longitudinal bar as number 1. UGWL data was collected by using each of these bars as the wave guide and taking a single reading in the center, at 9 inches from edges, as shown in Figure 23. Data representing each type of segment denoted by bars 3-7 are plotted in Figure 24. It can be seen that there is significant difference in the amplitude of the leaked waves between a completely intact membrane (bars 6 and 7) and those that experience physical separation due to anomalies: bars 3, 4, 5 for (gravel, bubbles, or paper towel).

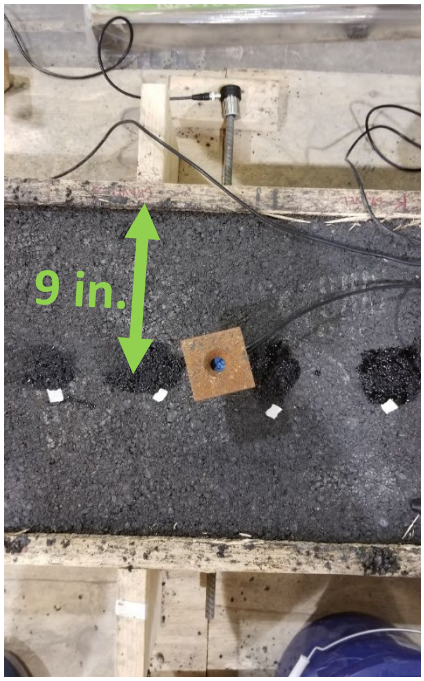

Figure 23. Transverse Bar UGWL Test Setup

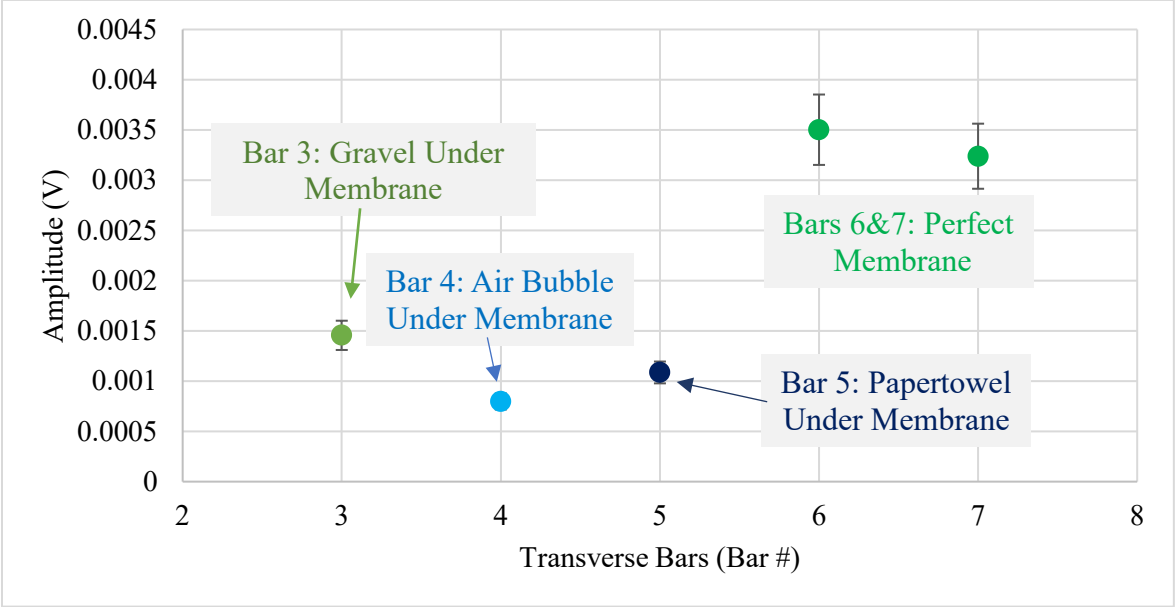

Figure 24. Transverse Bar UGWL reading results

Segment by Segment Analysis

Finally, to better evaluate the impact of the embedded flaws on the ultrasonic measurement, data is also collected by placing the transmitter at the start of each segment on the asphalt and measuring only for the

length of each segment (Figure 25). This allows the stronger range of the ultrasonic energy propagation to be used to examine each area.

The descriptions of segments and sensor placements used in this investigation are presented in Table 3. These sensor locations always refer to the left-most end of the entire specimen as the origin. Once all testing was completed, the specimen was dissected to correlate the data to the actual status of the embedded flaws at the membrane level (Figure 26). Segment by segment dissection photographs and the UPV test results are presented in Figures 27-38.

TABLE 3. Description of the Test Segments and First Two Data Point Results

Segment ID	Start & End	Test Area Description	Transmitter Location	Receiver Locations
B1	0"-24"	22" Perfect Membrane 1" Gap in membrane Next membrane (with gravel) for 1”	2"	6" 12" 18" 24"
B2	24"-48"	1" Gap (22"-23") 23" Gravel (23"-46") 2" Gap (46”-48”)	20"	24" 30" 36" 42" 48"
B3	48"-66"	1" Gap (46”-48”) 8" Bubble wrap in center of 18” long area	44"	48" 54" 60" 66"
B4	66"-84"	1" Gap (66”-67”) 17" Paper Towel	62"	66" 72" 78" 84"
B5	84"-End	3” Gap (84-87”) Perfect Membrane to End (87”-114”)	80"	84" 90" 96" 102" 108" 114"

Figure 25. Segment by Segment Indirect UPV Testing of Specimen B

Figure 26. Dissecting Specimen B to evaluate the asphalt-membrane-concrete interface

Segment B1 is one of the two "perfect membrane" sections in that there are no intentional flaws embedded in this area, which is 22 inches long (Table 3). Figure 27 shows the state of this membrane after the top asphalt layer is removed and the specimen is sliced.

Figure 27. Segment B1: Perfect Membrane 0-22" and 2" Gap 22-23".

Figure 28 shows the indirect UPV data from this section, which shows a typical attenuation and no abnormal increases/drops in the amplitudes.

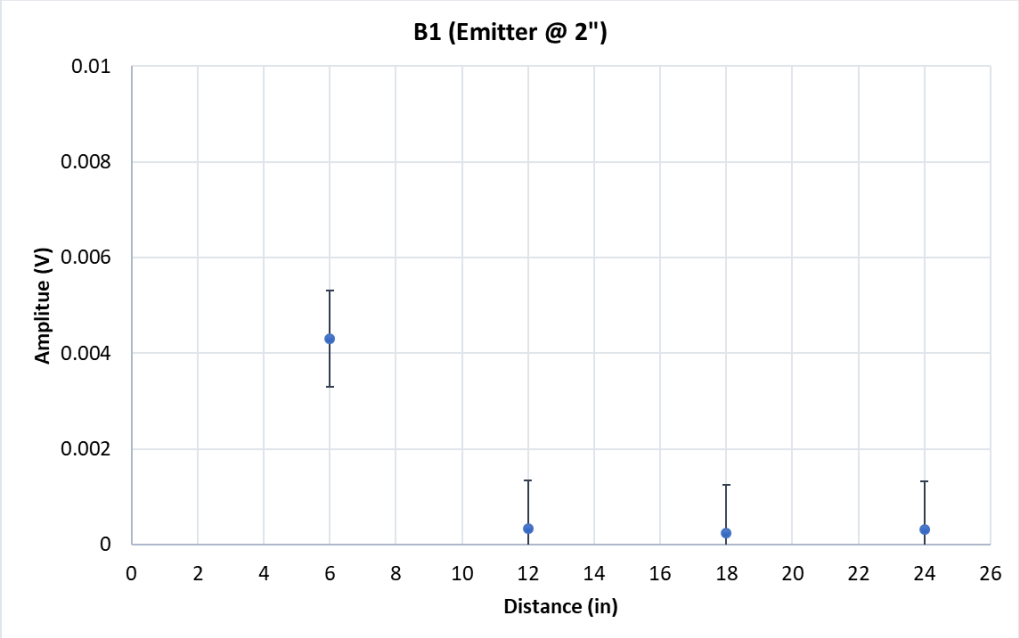

Figure 28. Segment B1 Indirect UPV results. Data attenuates as expected.

Segment B2 starts at 23 inches from the left end and it is where gravel was placed under the membrane (Table 3). Figure 29 shows the placement of the gravel under the membrane and Figure 30 shows the status of this area after the specimen was dissected.

Figure 29. Segment B2: Placement of the gravel under the membrane

Figure 30. Segment B2: Status of Membrane After Testing

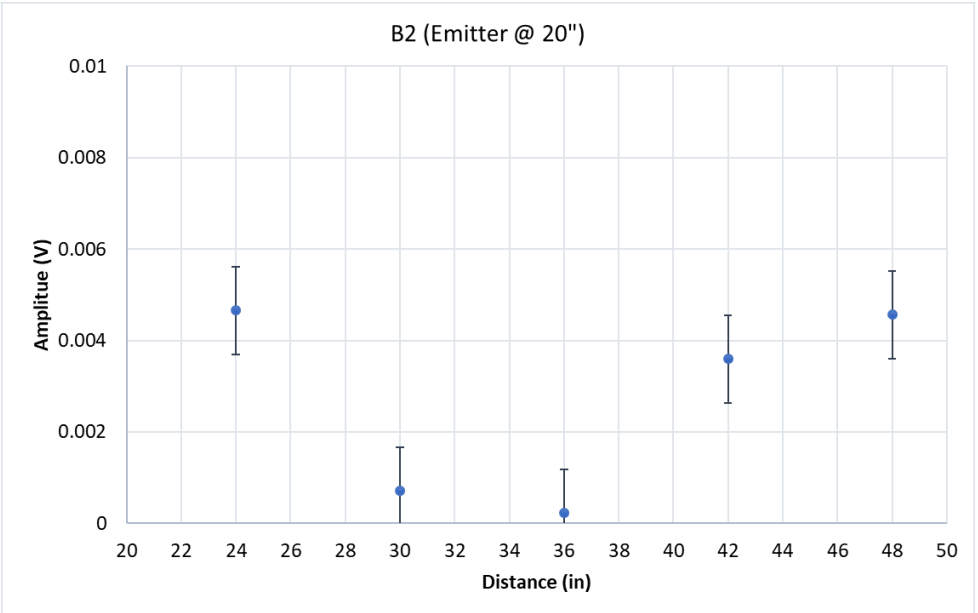

Figure 31. UPV test results on Segment B2.

Figure 31 shows the results of the UPV test on Segment B2 with the gravel under the membrane. As can be seen, the energy initially attenuates as expected, however, there is an increase in the amplitude at 42 inches from the left end of the specimen. The closeup photos of the studied specimen (Figure 30) shows that the membrane and primer bonded to the concrete strongly despite the gravel in most areas, but there are spots of delamination including one at 42 inches.

Segment B3 is where a bubble wrap was placed under the membrane. It was expected that the plastic would melt under the high heat of the asphalt and what will remain is the air bubbles. However, the dissection after the testing revealed otherwise: the bubble wrap was intact and created a physical separation between the membrane and the primer/concrete as can be seen in Figure 32.

Figure 32. Segment B3: Status of Membrane After Testing

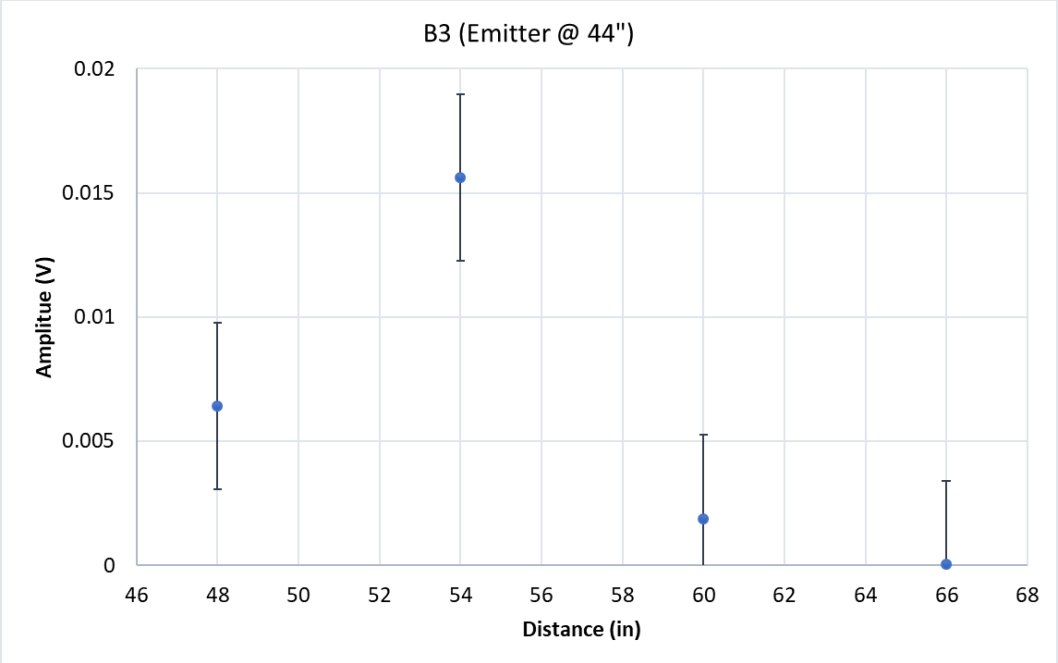

Figure 33. UPV test results on Segment B3.

Figure 33 shows the results for Segment B3. The spots of larger delamination results in much higher amplitudes, because the distance for the ultrasonic waves to travel became much shorter, spanning only the asphalt layer until the physical air gap. It should be noted that when Figure 32 and 33 are compared, the amplitudes are generally larger with the bubble wrap compared to the gravel area, once again confirming a continuous delamination with the bubble wrap insertion.

Segment B4 is where a moist paper towel was placed under the membrane. This insertion was intended to trap moisture under the membrane. While there is no direct evidence of moisture affecting membrane bond, the paper towel fibers appear to be embedded into the primer as shown in Figure 34. The results of this segment shown in Figure 35 indicate that this area does not necessarily register as an anomaly with the UPV tests and compared to Segment B3 amplitudes are generally lower.

Figure 34. Segment B4: Status of Membrane After Testing

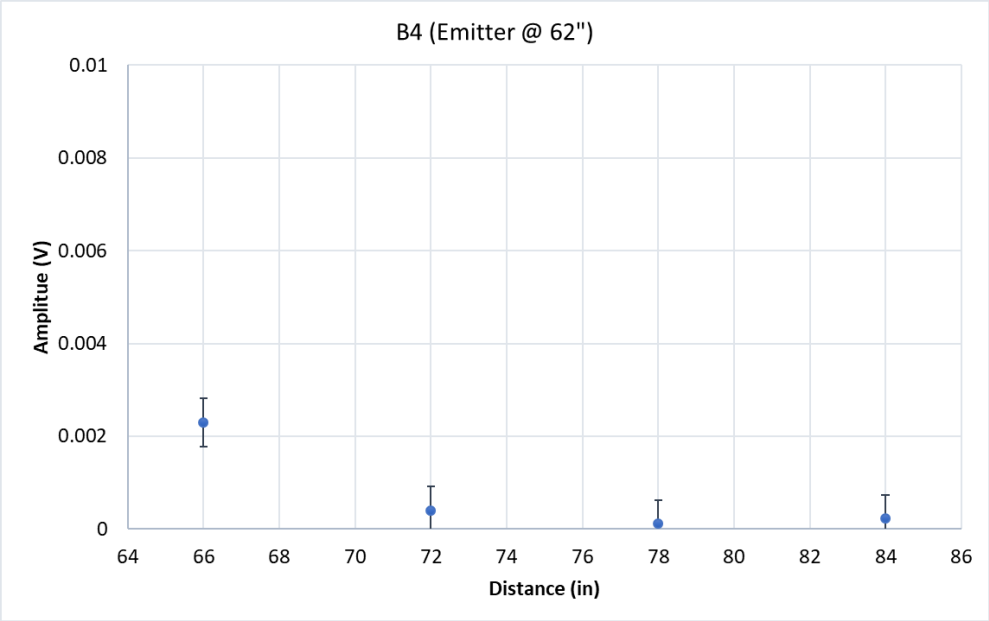

Figure 35. UPV test results on Segment B4.

Segment B5 is another perfect membrane segment with no intentional flaws embedded under (Figure 36). Results are expected that no abrupt increases or decreased in the data amplitudes are detected and the amplitudes are generally lower indicating a longer continuous path for the ultrasonic waves.

Figure 36. Segment B5: Status of Membrane After Testing

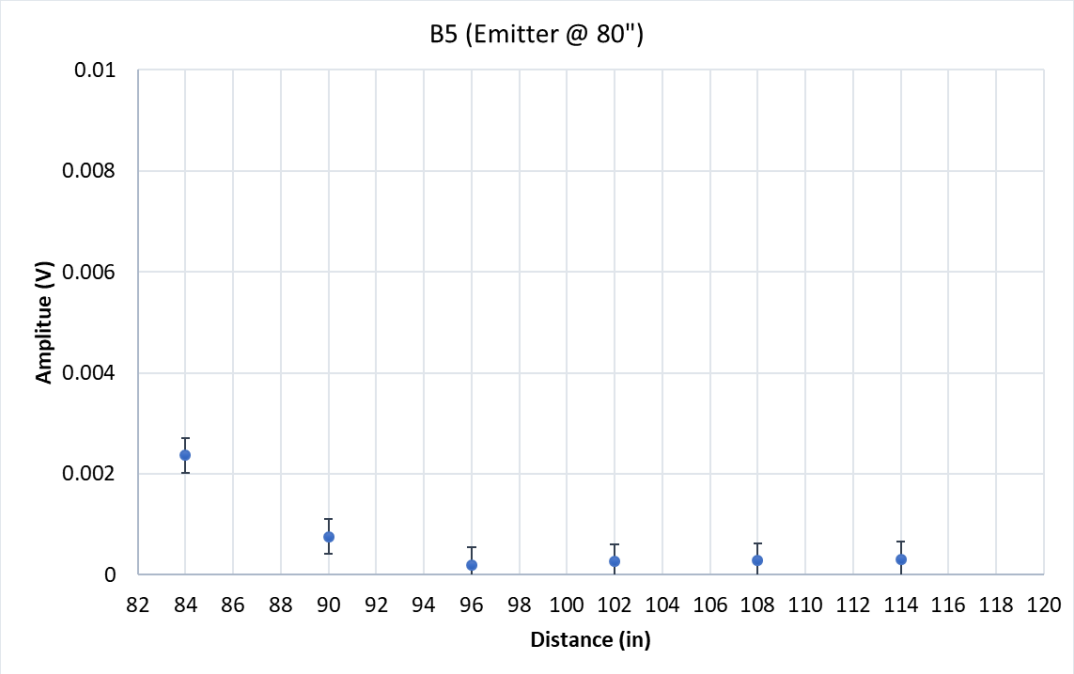

Figure 37. UPV test results on Segment B5.

Figure 38 presents these segment by segment analyses plotted together. Double points indicate the last read from a segment coinciding with the first reading of the next segment. This plot shows that the most obvious issues are at 42-66 inches, which spans the transition from the gravel to the bubble wrap areas.

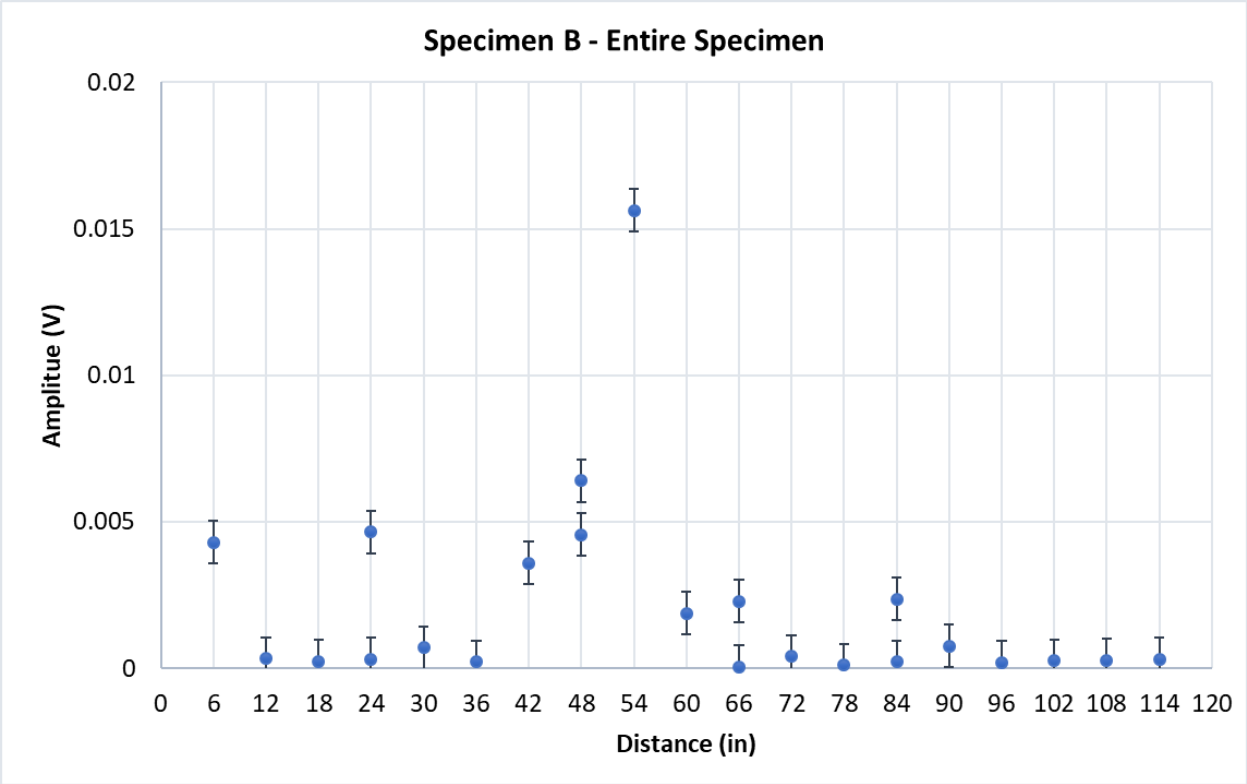

Figure 38. Segment by Segment Scans Plotted Together

When all of the studies on Specimen B are compared, following observations are made:

- Plots in Figures 19 and 24 are collected using UGWL method. Given this method send the energy through the rebar and measured the energy leaked into the surrounding medium, delaminations register as lower amplitudes and stronger bonds register as higher magnitudes.
- Figure 19 (UGWL through the longitudinal bar and single array reading) shows that despite being 7.5 ft away from the transmitter location on the rebar, the transition from the flawed areas to the perfect area could be clearly detected with an abnormal increase in the amplitudes.
- Figure 24 (UGWL through the transverse bars and individual readings for each bar) shows that when the readings over perfect membranes are compared to the readings over flawed membrane areas, results are as expected. As such, the transverse readings were also successful in identifying the anomalies but this method of measurement is more cumbersome.
- Figures 20, 21, 28, 31,33, 365, and 37 are results from the indirect UPV method application. In this method, the delaminations register as higher amplitudes as when there is a physical separation between the layers, the distance traveled decreases returning more of the energy to the receivers.

Therefore, both methods have been successful in detecting the anomalies at the membrane level with the largest notable results being the bubble wrap area with UPV and transition from the flawed areas to perfect membrane with UGWL. Further the UGWL method is more effective over longer examination distances for an "at a glance" understanding of the condition changes, but if higher accuracy is desired in determining the type and location of a flaw, it may be necessary to apply shorter range UPV testing.

4.3. Specimen Set C Results

Specimen Set C is used to study whether the corrosion in the rebar embedded in the concrete under the layers of asphalt, membrane, and primer can be detected. These specimens were cast earlier for NDOT Project M086 and for that project, Specimen C1 has been soaked in NaCl water for 6 months. It was confirmed that significant corrosion activity took place through chloride level testing (Erdogmus et al, report M086).

Figure 39 presents the UGWL test results for Specimen C1 where the transmitter is placed on the rebar and receivers are on the surface of the asphalt. The attenuation curve is as expected, indicative of a successful application of the UGWL method. However, when compared to UGWL results from before the asphalt was overlaid (Figure 39-bottom), as expected, the magnitudes are much lower. The peak amplitude for concrete-only readings is 0.11 versus 0.0025 because the leaked energy travels a much longer distance and through multiple layers (concrete, membrane, and asphalt).

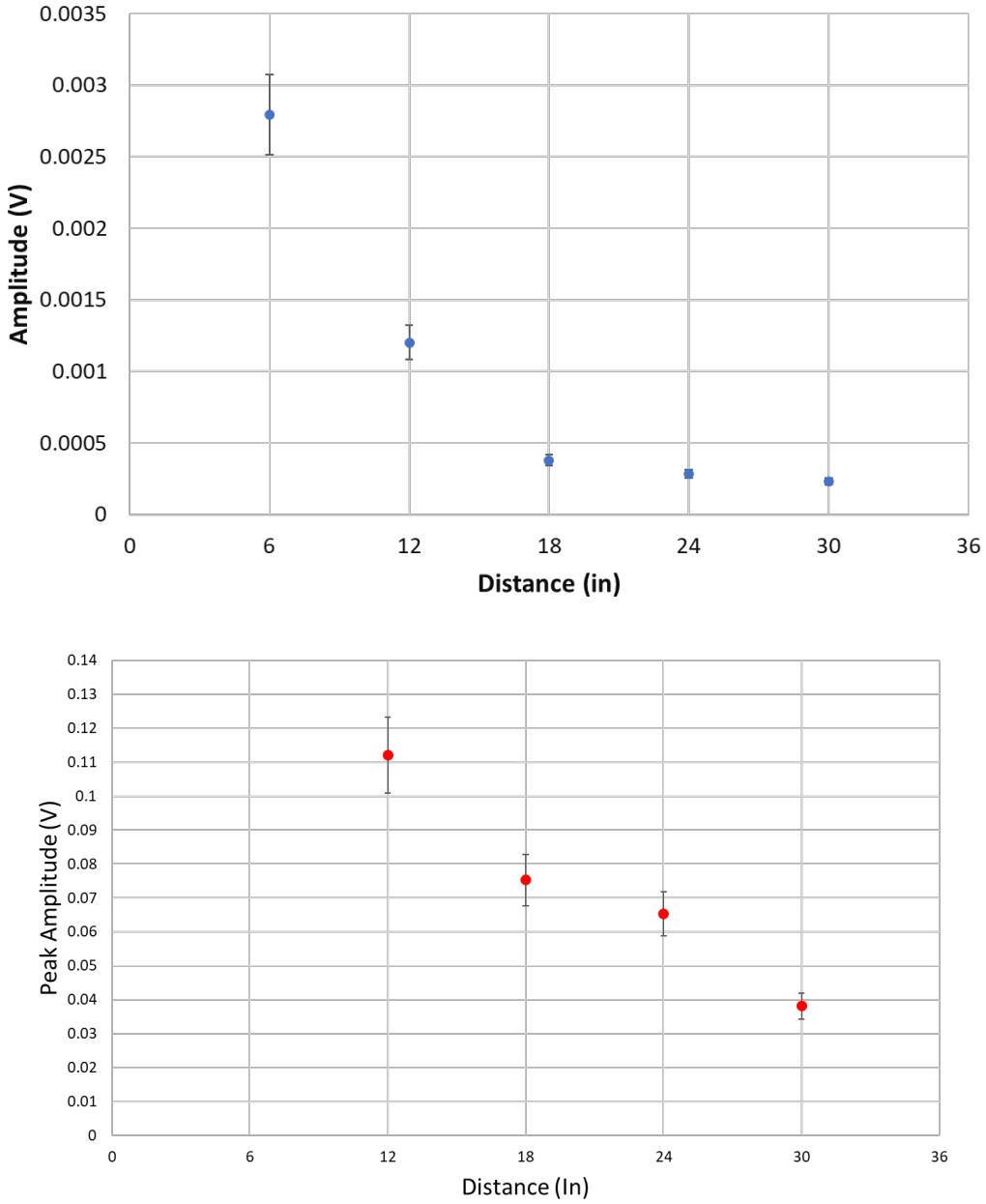

Figure 39. Top: UGWL Test Results on Specimen C1 After Asphalt Overlay: Conditioned rebar with blunt (0-degree end); Bottom: UGWL Test Results on Specimen C1 before Asphalt Overlay: Conditioned rebar with blunt (0-degree end)

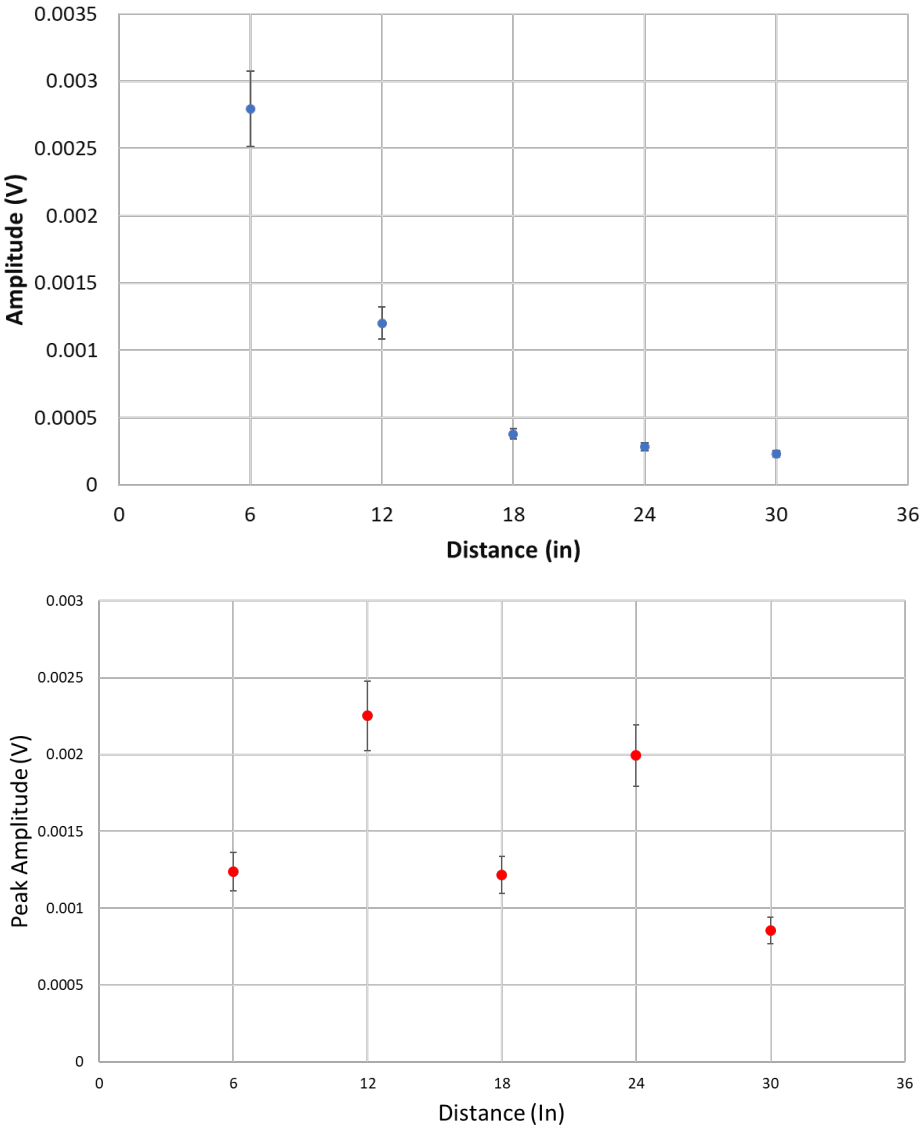

Figure 40. Left: Specimen C1 corroded rebar with 0-degree end, Right: Specimen C2 with clean rebar and 33-degree end.

Figure 40 compares the UGWL results from Specimen C1 with the corroded rebar at 0-degree-end (left) and Specimen C2 with the clean rebar at 33-degree end (right) after asphalt is overlaid on both specimens. The initial amplitudes for the corroded bar specimen are higher than the clean bar condition. This is expected from the UGWL method as reported previously (Erdogmus et al., 2020, M086 report). The early corrosion condition of Specimen C1 causes an increase in the leaked amplitudes due to the temporarily increased bonds between concrete and rebar. On the other hand, the data from Specimen C2 is more scattered and this is due to the bar end angle and deviations from the ideal UGWL method application (signals sent parallel to the bar).

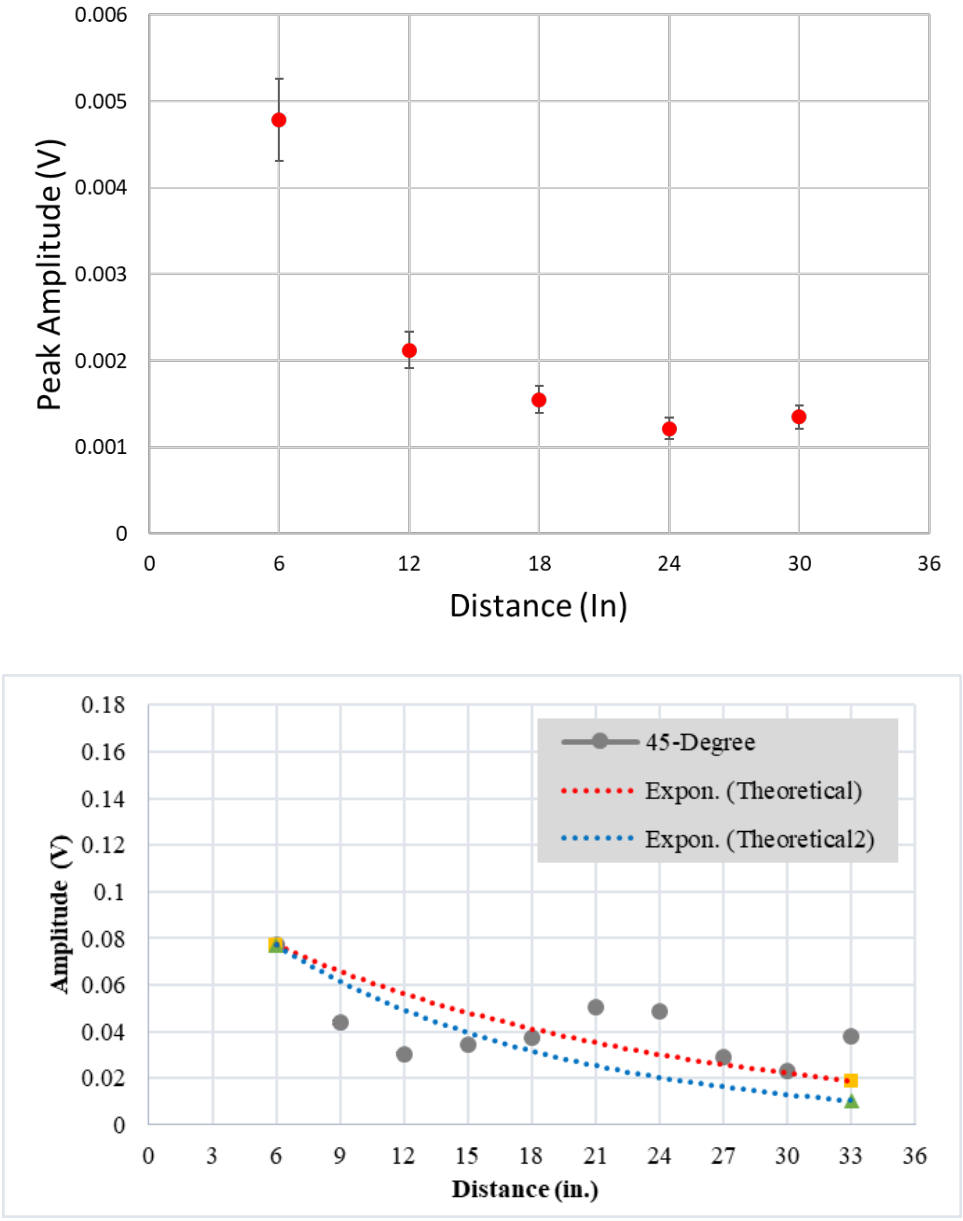

Figure 41. Top: UGWL Test Results on Specimen C3 After Asphalt Overlay. Bottom: UGWL Test Results on Specimen C3 before Asphalt Overlay

Figure 41 shows the results for Specimen C3. Once again, the method is applicable when the asphalt is added; however, the amplitudes are an order of magnitude smaller due to increased travel distance for the leaked waves and passing through three layers of materials.

4.4. Field Specimen Results

Figure 42 shows a view of the Field Specimen from the north end, and Figures 43 and 44 show the results when the waves are transmitted from of the Field Specimen for Rebars 2,4, 6, 8 and 9.

Figure 42. Field Specimen. View from North End showing the nine rebars

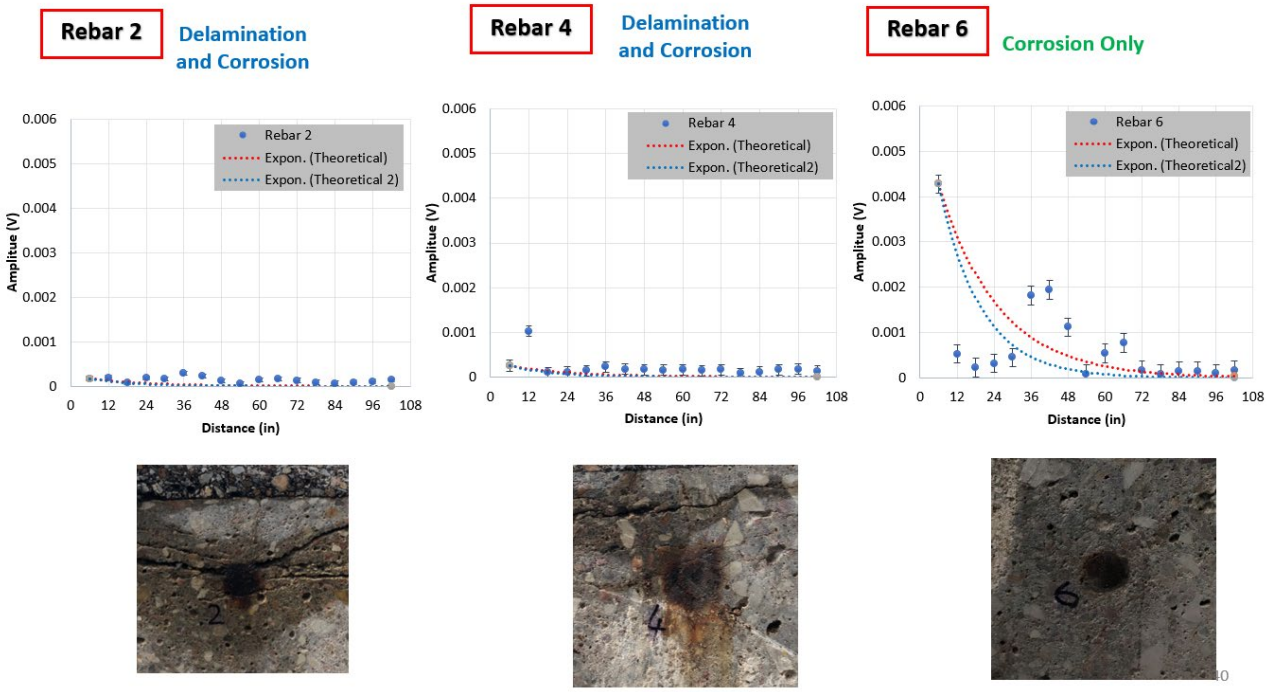

Figure 43. Field Specimen Results for Rebars 2, 4 and 6 from North End

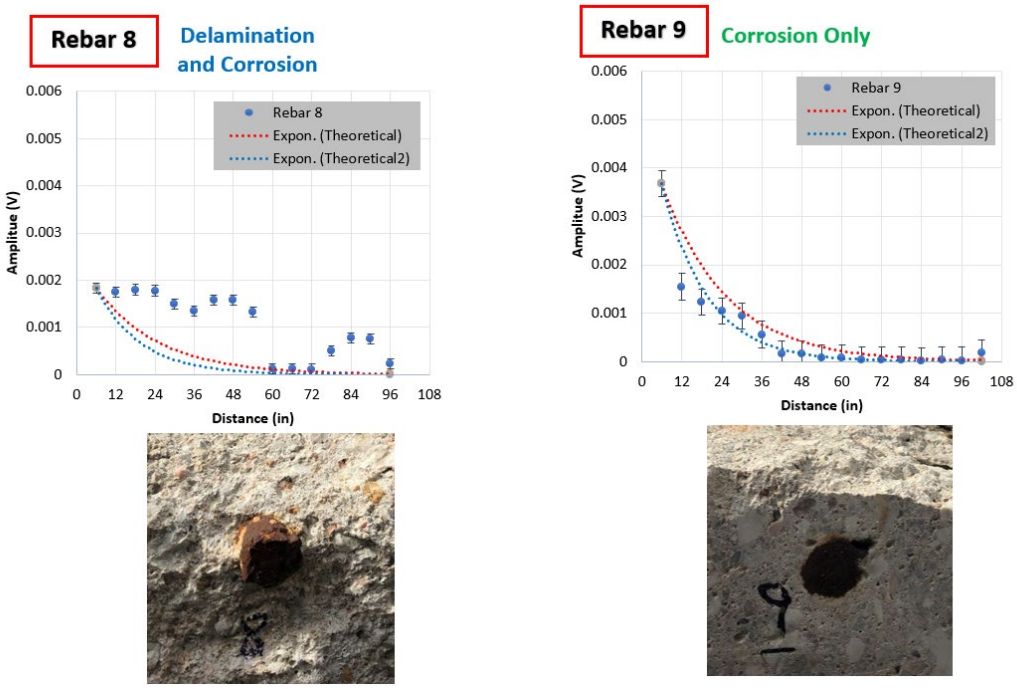

Figure 44. Field Specimen Results for Rebars 8 and 9 from North End

It can be seen in Figure 43 that when there is a large and visually discernible delamination between the rebar and concrete or within concrete, as in the case of Rebars 2 and 4, the starting amplitudes are relatively low. In contrast, when there is no visible delamination but corrosion, as in the case of Rebar 6 and 9, the starting amplitudes are 93-96% higher than rebars 2 and 4. In Figure 44, rebar 8 presents a different case where some of the concrete is spalled due to corrosion for the first half inch, but then it appears well-bonded to the concrete after that. The initial magnitude for this rebar is closer to those with the corrosion only bars, but 49-57% smaller.

Figure 45 shows a view of the Field Specimen from the north end, and Figures 42 and 43 show the results when the waves are transmitted from

Figure 45. Field Specimen. View from South End showing the nine rebars

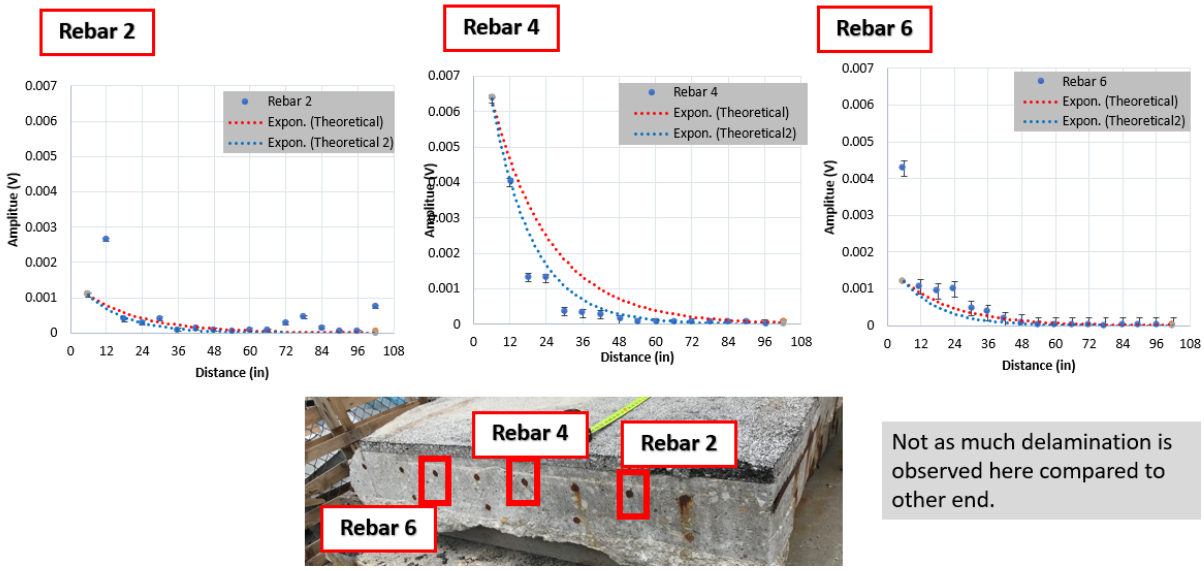

Figure 46. Field Specimen Results for Rebars 2, 4, 6 from South End

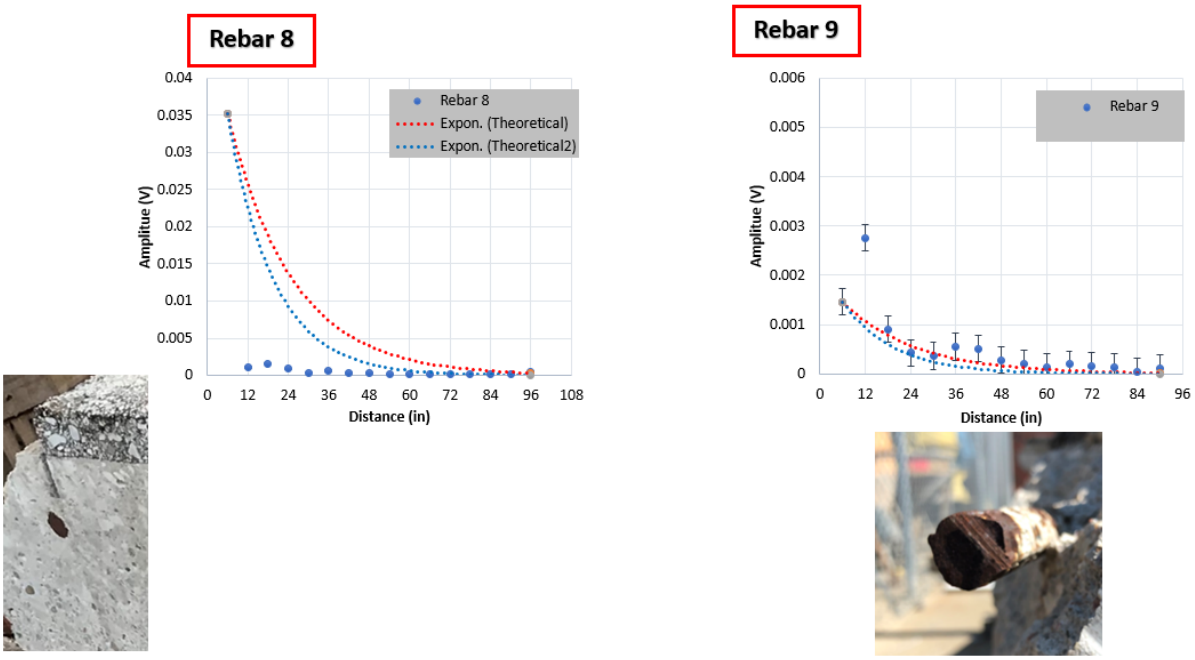

Figure 47. Field Specimen Results for Rebars 8 and 9 from South End

The strong correlation between the amplitudes and the condition of these different wave-guides presents a strong potential for the use of the UGWL method for condition assessment for rebars and rebar-concrete interphase in asphalt-overlaid reinforced concrete bridge decks, if the transmitter can be attached to the rebar. However, in this case, a solid set of baseline data from the newly constructed bridge is important to identify differences from that baseline condition. As stated in previous work on reinforced-concrete only specimens, the strength of the proposed UGWL method is as a continuous health monitoring method instead of an instantaneous measurement method.

5. CONCLUSIONS

Four different types of specimens were tested and the following conclusions are drawn from each set:

- Specimens A1 and A2 evaluated wave propagation in asphalt with and without an inserted rebar. , it was demonstrated that UGWL method can be successfully applied to asphalt if there is a bound element, like steel rebar, in the asphalt. Further, UGWL method provides amplitudes 10 times higher than UPV application; proving once again that the UGWL method provides higher sensitivity in measurements. However, it is not practical to count on metal bound elements inside the asphalt.
- Specimen B included various flaws at the membrane level but no known defects at the rebar-concrete interface. Specimen B shows strong potential for both the UGWL and segment-by-segment UPV methods to detect flaws at the membrane level. With longitudinal UGWL readings, the most significant data fluctuations observed were when the bond among the layers improved. When the transverse bars were used as wave guide, UGWL method could also differentiate between perfect membrane and flawed membrane regions. The segment-by-segment UPV testing also detected flaws, especially when the data is plotted together. Therefore, both methods (UPV and UGWL) have been successful in detecting the anomalies at the membrane level- but care must be taken to interpret the results. The increase and decrease in amplitudes indicate opposite results between the two methods.
- Specimen Set C was useful in studying whether or not flaws at the rebar level can be detected when the specimen is overlaid in asphalt. The significant differences in the amplitudes gathered from UGWL testing of specimens C1 versus C2 and C3 (i.e. corroded versus clean rebars) show that despite the smaller amplitudes compared to concrete-rebar only specimens, it is possible.
- Finally, the field specimen was an old existing bridge deck segment that had visible corrosion and delamination issues at the rebar and concrete interface. Significant UGWL amplitude changes were observed that correlated well to the visible condition of the rebar, rebar-concrete interface, and concrete layers.

Overall, this paper presents the proof-of-concept experimental results for the method's application to asphalt overlaid reinforced concrete specimens, which are significantly more complex. It should be reiterated that the strength of the proposed UGWL method is as a continuous health monitoring method instead of an instantaneous measurement method as the "change in amplitude" is more meaningful than the actual amplitudes, as the amplitudes depend on other factors such as attenuation (distance from the transmitter). It can be concluded that while further research is needed, there is *very strong potential for this method to answer an important gap in research and application in the field of bridge deck assessments*. If this method can be further developed for membrane inspections, it will be a very significant contribution to the field as it can help DOTs avoid costly corrosion issues and deck replacements/repairs.

ACKNOWLEDGMENTS

This research was funded by the Nebraska Department of Transportation (NDOT). Any opinions presented in this paper reflect those of the authors and do not necessarily represent those of the funding agency. The project team extends their gratitude to laboratory staff Peter Hilsabeck and Jose Lopezand students Shoaib Amiri, Khalid Alwashahi, Ethan Hall, and Dawson Langholdt for assistance with lab work; NDOT staff Mike Reynolds, Mike Vigil and Robert Rea for help with designing and casting the asphalt specimens; the NDOT TAC for their valuable technical feedback; and finally UNL faculty Dr. Jingying Zhu for sharing the field specimen.

REFERENCES

Amiri, S. A. (2020). A Comparison Between Ultrasonic Guided Wave Leakage and Half-Cell Potential Methods in Detection of Corrosion in Reinforced Concrete Decks, Master's Thesis, 2020.

Amiri, S.A., Erdogmus, E. Richter-Egger, D. (2021). A Comparison Between Ultrasonic Guided Wave Leakage and Half-Cell Potential Methods in Detection of Corrosion in Reinforced Concrete Decks, Signals Journal, MDPI, Accepted for Publication.

ASTM C597 (2016). Standard Test Method for Pulse Velocity Through Concrete. ASTM International.

Cui, J. (2012). Multiple Sensor Periodic Nondestructive Evaluation on Concrete Bridge Deck Maintenance. Thesis, University of Vermont, 2012.

Erdogmus, E; Garcia, E., Amiri, A., Schuller, M, (2020). "Prototype System for Implementing the Ultrasonic Guided Wave Method on the Field," NDOT Project Report, Report No. M086.

Erdogmus, E; Garcia, E., Amiri, A., Schuller, M, (2020). "A Novel Structural Health Monitoring Method for Reinforced Concrete Bridge Decks Using Ultrasonic Guided Waves," *Infrastructures*, 2020. 5(6).

Garcia, E., Erdogmus, E., Schuller, M., & Harvey, D. (2017). Novel Method for the Detection of Onset of Delamination in Reinforced Concrete Bridge Decks, *Journal of Performance of Constructed Facilities*, 2017, 31(6), 04017102.

Garcia, Eric, Erdogmus, E., Schuller, M., & Harvey, D. (2019). Detecting Onset of Different Types of Flaws in Reinforced Concrete, *ACI Materials Journal*, 2019. 116(1).

Haser, A. N., McGovern, M. E., Behnia, B., Buttlar, W., & Reis, H. (2015). Monitoring viscosity in asphalt binders using an ultrasonic guided wave approach. Insight-Non-Destructive Testing and Condition Monitoring, 57(4), 212-220.

Hoegh, K., Khazanovich, L., Maser, K., & Tran, N. (2012). Evaluation of ultrasonic technique for detecting delamination in asphalt pavements. Transportation Research Record, 2306(1), 105-110.

Khazanovich, L., Velasquez, R., & Nesvijski, E. G. (2005). Evaluation of top-down cracks in asphalt pavements by using a self-calibrating ultrasonic technique. Transportation research record, 1940(1), 63-68.

McGovern, M. E., Buttlar, W., & Reis, H. (2018). Evaluation and Life Extension of Asphalt Pavements Using Rejuvenators and Noncollinear Ultrasonic Wave Mixing: A Review. Journal of Nondestructive Evaluation, Diagnostics and Prognostics of Engineering Systems, 1(1), 011002.

Pahlavan, L., Mota, M. M., & Blacquière, G. (2016). Influence of asphalt on fatigue crack monitoring in steel bridge decks using guided waves. Construction and Building Materials, 120, 593-604.

Tigdemir, M., Kalyoncuoglu, S. F., & Kalyoncuoglu, U. Y. (2004). Application of ultrasonic method in asphalt concrete testing for fatigue life estimation. NDT & E International, 37(8), 597-602.

Yunovich, M., N. Thompson, T. Balvanyos, and L. Lave. (2001). Corrosion Cost and Preventive Strategies in the United States, Appendix D—Highway Bridges. *Publication FHWA-RD-01-157. Federal Highway Administration*, 2001.

Zargar, M., Banerjee, S., Bullen, F., & Ayers, R. (2017, July). An Investigation into the Use of Ultrasonic Wave Transmission Techniques to Evaluate Air Voids in Asphalt. In Global Civil Engineering Conference (pp. 1427-1439). Springer, Singapore.